224 F

Using Static Pushover Analysis To Determine The Ultimate Limit States Of Gulf Of Mexico Steel Template-Type Platforms Subjected to Hurricane Wind and Wave Loads

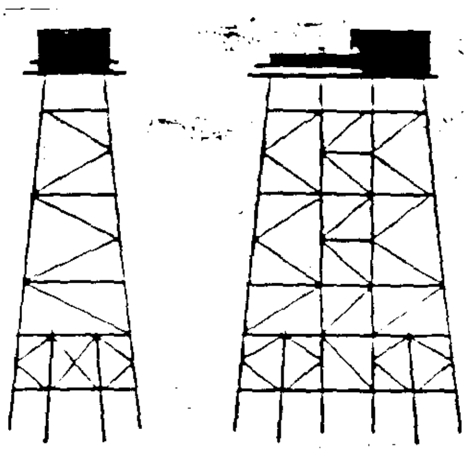

by

James D. Stear

and

Professor Robert G. Bea

Report to

U.S. Minerals Management Service

and

Joint Industry Project Sponsors

Marine Technology and Management Group

epartment of Civil and Environmental Engineering

University of California at Berkeley

March 1996

ABSTRACT

The purpose of this study was to determine with what degree of accuracy a steel template-type offshore platform's ultimate limit state behavior under hurricane wind and wave loads can be predicted by using static pushover methods. Ultimate limit state evaluations were performed on two Gulf of Mexico platforms subjected to hurricane wind and wave conditions. These evaluations were compared with historical platform performance during storms and results from previous analyses performed by others. In addition, the effects of pile foundation modeling, of bracing member imperfection, and of horizontal framing members on platform strength were examined analytically.

TABLE OF CONTENTS **Page**

1.0 INTRODUCTION

There exist today over 3,800 steel template-type offshore structures in the Gulf of Mexico, sited in water depths ranging from a few fathoms to over 1,000 feet. Many of these structures were designed in the 1950's and 1960's to much lower wave heights and load levels than are prescribed in current codes for the design of new platforms. With these aging structures being called upon to serve beyond their original design life, the need has arisen for accurate means of assessing their ability to survive environmental conditions much more severe than those originally considered.

For the past three years, the Marine Technology and Management Group (MTMG) at U.C. Berkeley has performed a series of research projects, sponsored by regulatory agencies and platform owners, intended to develop and refine analytical screening methodologies that can be used to assess the suitability of aging offshore structures for continued service. This research has concentrated primarily on the development and use of ultimate limit state (ULS) analysis techniques for the purpose of screening steel template-type platforms in the Gulf of Mexico subjected to hurricane wind and wave forces. Parts of the research effort have been directed towards the development of "simplified" ULS analysis procedures (Mortazavi, Bea, 1994), while other parts have focused upon performing detailed ULS evaluations of typical platforms using current analysis methodology and existing non-linear analysis software (Loch, Bea, 1995). This latter effort has concentrated on verifying the suitability of using detailed static pushover analyses to make accurate assessments of a given platform's ULS behavior, and to identify conservatisms, load and structural effects not accounted for, as well as general difficulties in the performance of these analyses which may skew or bias the results away from actual platform behavior.

This report represents a continuation of the effort documented by Loch and Bea (1995). ULS evaluations of two additional steel template-type structures subjected to hurricane wind and wave loads, Shell South Pass 62A and Shell Ship Shoal 274A, have been performed using static pushover analysis. The ULS behavior of each structure as predicted by the analyses is compared with platform historical data. In addition to these ULS evaluations, two analytical issues, namely the difficulties of modeling imbedded pile behavior and the effects of member imperfection on the ULS, have been discussed. Furthermore, the effect of horizontal framing members within jacket structures on ULS behavior is examined. Lastly, general difficulties which arose during the performance of these detailed analyses are identified and discussed, and suggestions as to how improvements might be made to the analysis process are mentioned.

1.1 Purpose and Scope

This study has two primary goals. The first is to continue the effort begun by Loch and Bea (1995) in verifying the utility of static pushover analyses in accurately assessing the ULS performance of steel template-type structures subjected to hurricane wind and wave loads. This includes not only performing additional verification studies, but also examining areas of the analysis process which may be conservative or extremely sensitive to input. The second goal is to provide detailed results on typical platform ULS behavior for use in calibrating and verifying the program ULSLEA (Mortazavi, Bea, 1994), which has been developed as part of the simplified ULS analysis screening effort.

Static pushover analyses have been performed using SINTEF's USFOS program (SINTEF, 1994) for two additional steel template-type structures, Shell South Pass 62A and Shell Ship Shoal 274A, for load patterns consistent with those of hurricane wind and wave loads. Information on each platform's structure and equipment was provided by Shell. The results of these analyses are compared to data on actual platform performance collected following extreme loading events; SS274A survived Hurricane Hilda in 1964 with moderate damage, while SP62A survived Hurricane Camille in 1969 with no significant structural damage. The analyses performed have restricted wave attack to the principal directions only (end-on and broadside). The reader is referred to Loch and Bea, (1995) for more detailed information concerning the analysis methodology and program system utilized in the performance of these evaluations.

It should be noted that no dynamic effects have been explicitly considered in these analyses (Bea, Young, 1993). Geometric (i.e. stress concentrations) or material imperfections which might lead to cracking or brittle fracture have not been evaluated. Local member failures such as shell buckling and tearing have not been explicitly considered.

Two issues addressed within this report, those of the modeling of the foundation piles and the effects of member imperfection on ULS behavior, are continuations of studies started by Loch and Bea (1995). The reader is referred to this report for further details concerning these studies. Results from both SP62A and SS274A are discussed with respect to the modeling of the foundation piles, while the model for SP62A was used to evaluate the effects of member imperfection on ULS. The evaluation of the effects of horizontal framing on ULS behavior is a new study intended to verify a key assumption in the program ULSLEA approach (Mortazavi, Bea, 1994) involved with determination of the lateral capacities of jacket bays. The assumption is that whether or not there is framing above and below the jacket bay, first member failure in the bay will be unaffected. The model for SP62A was used to perform this latter study.

1.2 Organization of Report

This report is divided into four sections. The first section provides general background on the purpose and scope of the project which has sponsored this report. The second section contains the results of the ULS verification analyses of SP62A and SS274A, as well as comparisons of these results with historical data. The third section contains the results of several parametric studies involving the modeling of foundation piles, the effects of member imperfection on ULS, and the effects of horizontal framing on ULS. The fourth section contains a brief summary of the results of the verification studies, and comments upon various difficulties encountered during the analysis process. Recommendations for areas of future study are also made.

1.3 Acknowledgments

This project was sponsored by the U.S. Minerals Management Service in cooperation with the California State Lands Commission. The parallel project to develop and verify ULSLEA (Mortazavi, Bea, 1995) was sponsored by ARCO Exploration and Production Technology, Exxon Production Research Company, Mobil Technology Company, Shell Offshore Incorporated, and Unocal Corporation.

Special appreciation is expressed to Shell Offshore Incorporated, Mr. Kris Digre and Dr. Rabi De, for the data and information on SP62A and SS274A.

2.0 VERIFICATION CASES

This section presents the results of the static pushover analyses of SP62A and SS274A. The general procedures used in the analyses are first summarized; subsequent sections describe each platform evaluation. For each platform, a description of the structure is given, along with a description of the structural model and load characteristics. Collapse load and failure mode have been identified for the principal directions of loading (end-on and broadside). Comparisons of the analysis results are then made with historical data on the platforms.

2.1 Analysis Procedures

The platforms studied were modeled using DNV's PREFRAME program (DNV, 1994a). Only the major structural components were included within the models; the contribution of appurtenances and conductors to the platforms' stiffnesses and strengths were neglected. However, loads induced on the platforms due to these "non-structural" components were taken into account. Foundation pile behavior was taken into account through the use of non-linear spring-to-ground elements.

For each platform, wind, wave and current conditions were established in accordance with API RP 2A Section 2.3.2 and Section 17 (API, 1993, 1994). Jacket and conductor loads were generated using DNV's program WAJAC (DNV, 1994b); WAJAC computes loads on members using the Morison formulation. Deck loads due to wind and wave forces were calculated in accordance with the methods outlined in API RP 2A Section 2.3.2 and Section 17 (API, 1993, 1994). For each platform, only the principal directions of loading (end-on and broadside) were considered; it was judged that these results should bound the true ULS of each structure in so far as failure in the jacket and/or deck legs was concerned.

The static pushover analyses were performed using SINTEF's USFOS program (SINTEF, 1991, 1993, 1994). USFOS is a very capable advanced state-of-the-art analysis program designed to perform collapse analysis of steel offshore structures. Its solution procedure accounts for both geometric and material non-linearities. USFOS incrementally increases the load on the structure until collapse in achieved or until a global instability (such as a member buckling) occurs. In the case of global instability, the load is reduced until equilibrium is regained, at which point the load is increased again.

For each analysis, the wave height used in determining the collapse load was adjusted until a load factor of unity was achieved. Wave forces on decks and appurtenances were recalculated for each wave height using water particle kinematics appropriate to the deck and appurtenance locations. It was felt using the wave load which resulted in a load factor of unity was much more appropriate than simply increasing a lower initial wave load until collapse was achieved; the latter approach leads to concentration of forces in the lower portions of the jacket, which may result in missing the actual failure mode of the platform.

Data from the analyses was collected and processed using SINTEF's POSTFOS program (SINTEF, 1992). POSTFOS extracts data selected by the user for global, element and nodal force/displacement histories, and saves them in spreadsheet form so that they may be easily manipulated by the user. Use was also made of SINTEF's graphical postprocessor XFOS (SINTEF, 1992) to quickly view results of the analyses and study the progress of the solution. The preprocessing, analysis and data collection were all performed on an IBM RISC 6000 computer. Some data reduction and graphics work was performed on an Intel Pentium machine using the spreadsheet Microsoft Excel 5.0.

For additional information on the program system used, and the general methodology and theoretical background of the loadings and analysis, the reader is referred to Loch and Bea (1995).

2.2 South Pass 62A

2.2.1 Platform Characteristics

SP62A is one of three similar platforms located in the South Pass region of the Gulf of Mexico off Louisiana. It was installed in 1967. The platform is an 8-leg jacket structure sited in 340 ft of water (see Figure 2.2.1-1). It is classified as an unmanned drilling and production platform, and it supports 18 24 inch-diameter conductors. The platform was originally designed in 1966 for a 58 ft wave with 4 ft/sec current, and Morison drag and inertia force coefficients of 0.5 and 1.5, respectively (Tromans, van de Graaf, 1992).

SP62A has decks at +45 ft and +60 ft MGL (mean Gulf level). The base dimensions of the jacket are 202 ft x 122 ft, with the long dimension running

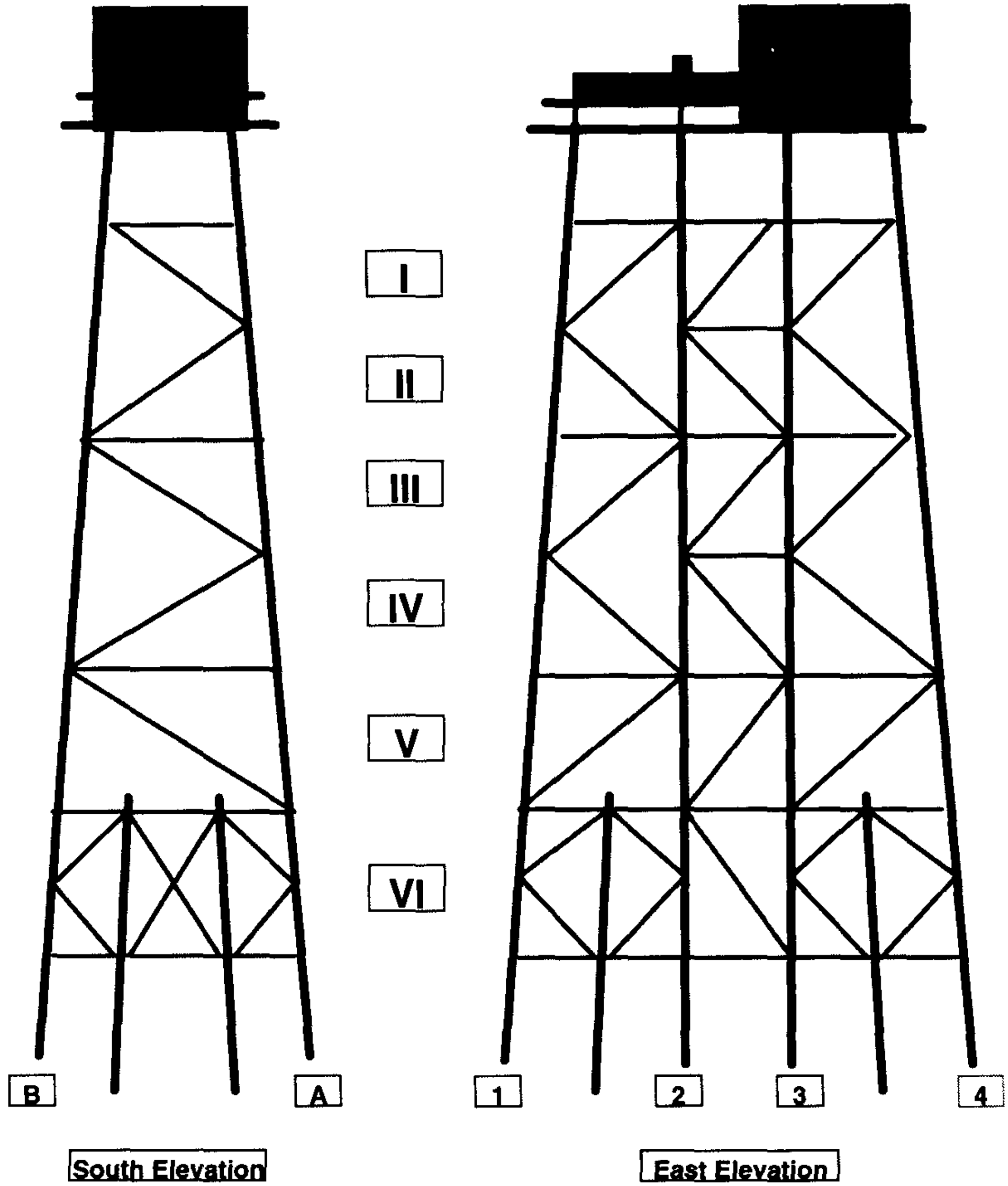

Figure 2.2.1-1: South Pass Block 62 Platform Elevations

NNW-SSE. The perimeter framing of the jacket is battered to 1:10. The jacket legs are fabricated from sections ranging from 53 inches in diameter (w.t. 0.625 inch) to 54 inches in diameter (w.t. 1.5 inches). The skirt guides are 56 inches in diameter (w.t. 0.625 inch). Braces in the jacket range from 30 inches in diameter (w.t. 0.625 inch) in the lower bay to 24 inches in diameter (w.t. 0.5 inch) in the top bay. Most of the major joints in the jacket are canned, with the cans and brace ends (typically 5 ft on either end) fabricated from A441 steel as opposed to A36, which constitutes the majority of the jacket and piles.

The foundation consists of 8 main piles and 8 skirt piles. The main piles are 48 inches in diameter (w.t. from 0.625 inch to 1.125 inches); they pass through the legs and are welded off at +20 ft MGL. The deck legs are 48 inches in diameter (w.t. 1.0 inch) and are welded to the tops of the main piles. The skirt piles are also 48 inches in diameter (w.t. from 0.625 inch to 1.25 inches), and are grouted in their guides in the bottom jacket bay. All piles were driven to 180 ft penetration. Information on the soil conditions was provided by Shell. Based on on-site soil borings, the soil profile has been characterized as:

0-12	ft	silty fine sand with clay seams
12-60	ft	silty sand (dense)
6-90	ft	fine to medium sand (dense)
90+	ft	fine to silty-fine sand

As noted previously, the deck legs, jacket members and the piles are made primarily from A36 steel. The mean strength of the A36 material has been taken to be 43 ksi. This increase accounts for the differences between the mean and minimum specified yield strengths, and for strain rate effects associated with the wave loadings (Galambos, Ravindra, 1978; Nadai, 1950).

2.2.2 Platform History

In 1969 Hurricane Camille passed over the South Pass region, subjecting SP62A and its sister platforms (SP62B and C) to very severe wind and wave loads. Measurements and inferences from displaced equipment indicate that SP62A was struck by both 72 ft- and 75 ft-high waves, both of which struck and inundated the lower (+45 ft MGL) deck of the platform (Bea, 1975). Nearby, SP62B was struck by a wave between 76-78 ft high, and suffered some minor damage to the lower deck and some equipment (Bea, 1975). SP62C was loaded by a wave between 68-71 ft high based on platform damage and wave height measurements (Bea, 1975). It is remarkable in light of the fact that while each of these platforms was designed for a wave height of 58 ft, they all survived these extreme loads without any noticeable structural damage. All of these platforms are in service today.

2.2.3 Structural Model of Platform

The analytical model developed for SP62A contains the major structural components of the platform (see Figures 2.2.3-1,2,3). It was assumed the deck structural members would not fail; hence only the main framing members of the deck were included. Inelastic deformation of the deck members was suppressed. The conductor framing was included in the model, but the conductors themselves were modeled as four sets of "equivalent" conductors, with a diameter sized such that the Morison drag load generated on each equivalent set would be equal to the load generated on 4.5 of the original conductors. It should be noted that this procedure will result in overprediction of the Morison inertia load generated on the conductors, but as the peak load on the platform occurred when the crest of the wave was near the midsection of the structure (and hence water particle accelerations are close to zero) it was judged this error would be minimal. The conductor elements were declared non-structural elements so as not to contribute to the global stiffness of the platform.

Brace elements in the jacket were given a single curvature imperfection equal to 0.0015L, with deformation conservatively assigned in the direction of the load (see Figure 2.2.3-4). The value of 0.0015L is suggested as giving good results with the Lehigh University design buckling load vs. reduced length factor curves (SINTEF, 1991).

Imperfections were only assigned to elements for a specific load case if those elements were identified as being part of the failure mode from an initial "trial" analysis in which no imperfections were assigned. No imperfections were

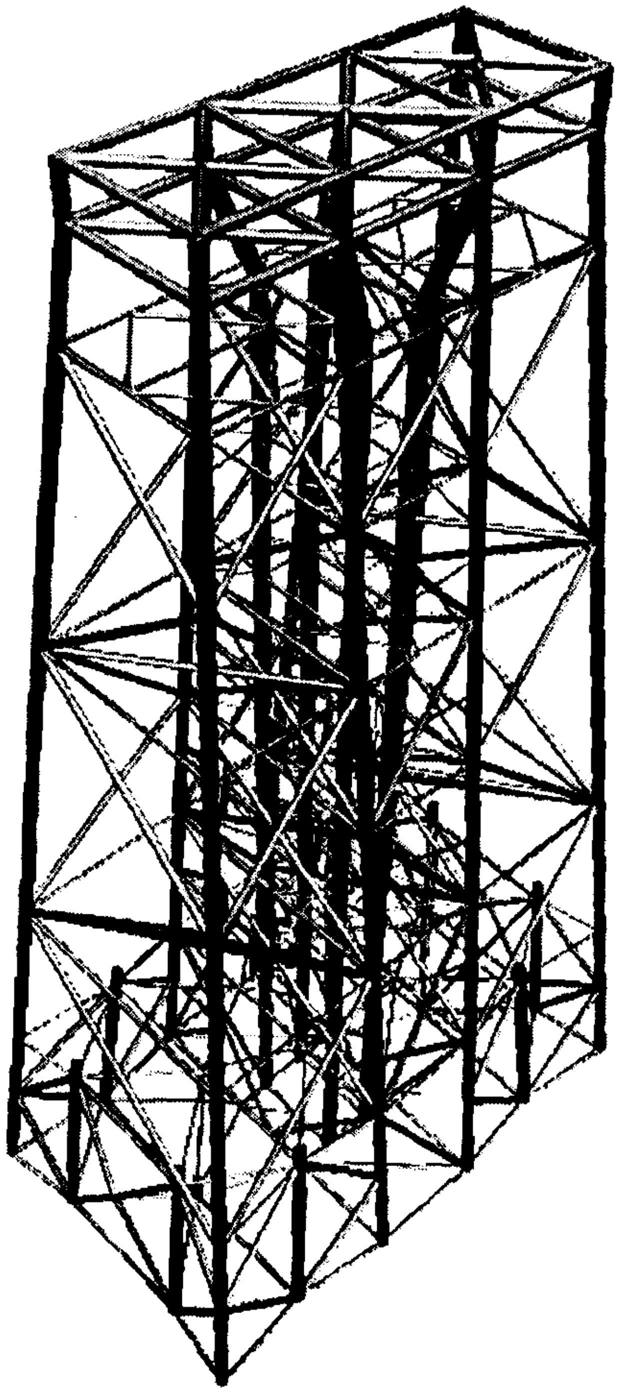

Figure 2.2.3-1: South Pass Block 62 Platform Isometric

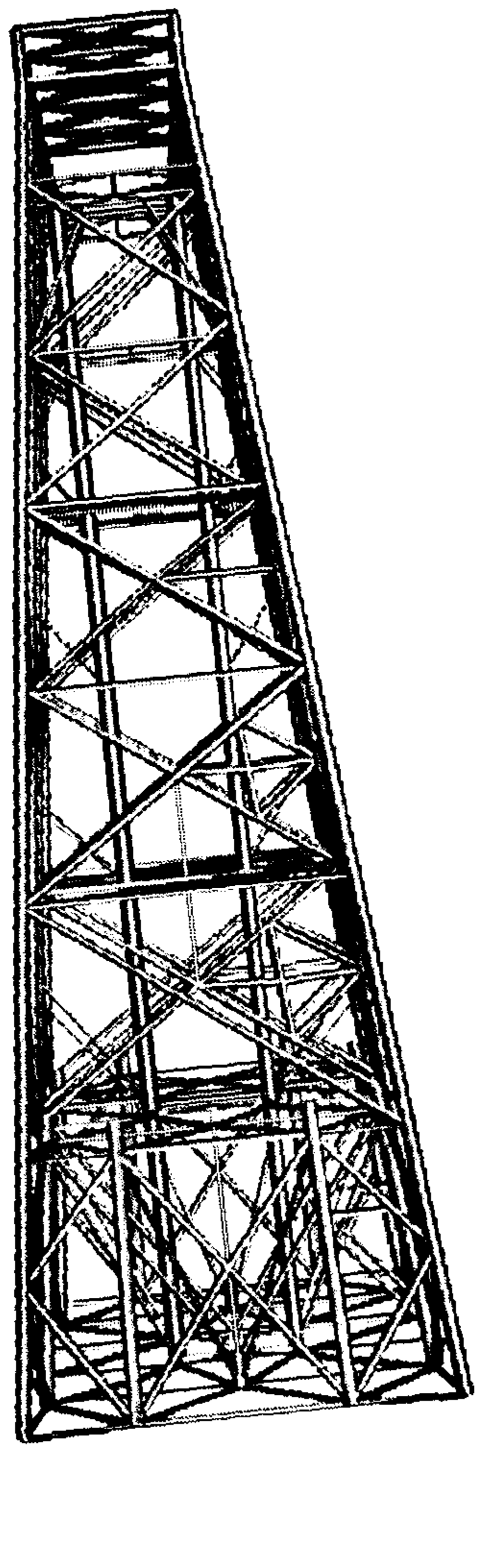

Figure 2.2.3-2: South Pass Block 62 Platform South Elevation

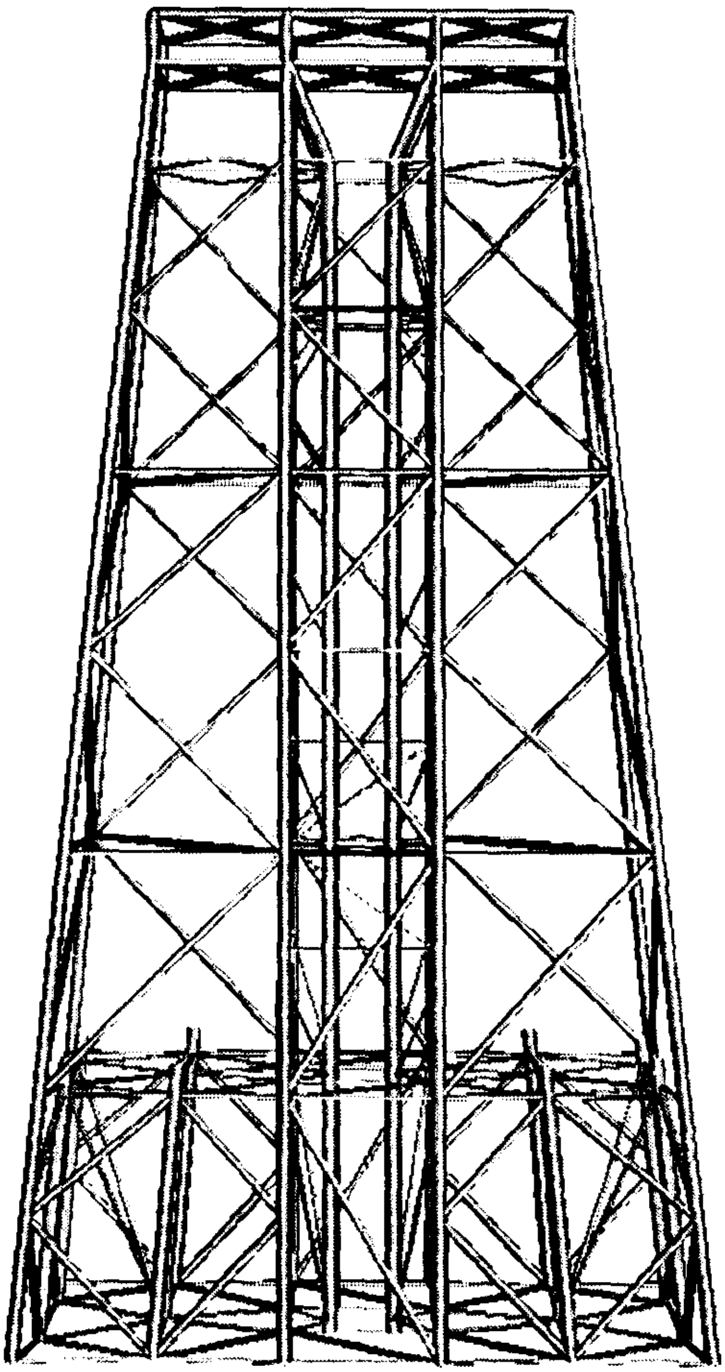

Figure 2.2.3-3: South Pass Block 62 Platform East Elevation

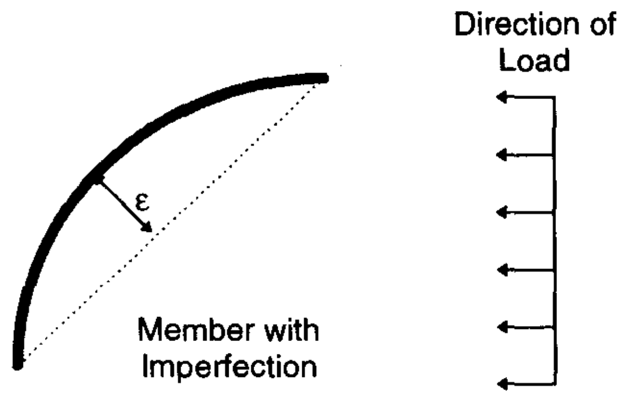

Figure 2.2.3-4: Imperfection Orientation

assigned to the jacket legs, as these members were expected to fail well after the majority of the bracing had failed, and hence after the collapse load had already been reached.

The analysis was performed assuming rigid joints. The joints are comprised of heavy wall branch and chord cans. Evaluation of joint capacities and stiffnesses indicated that the assumption of rigid joints was reasonable.

The main piles above the mudline were modeled discretely from the jacket sleeves, with the two constrained together for the purposes of lateral displacement. The skirt piles above the mudline were lumped together with their guides into a single element due to the fact the skirts were grouted in their guides.

To characterize the behavior of the piles below the mudline, it was decided to use the response of a single detailed pile-soil model to unit loads in order to generate a series of force-displacement relationships which could be used with the USFOS non-linear spring-to-ground element. These springs would then be attached to the ends of the piles terminating at the mudline, thus simulating appropriate foundation behavior. A model of a single unbattered pile-soil system was developed (it was felt the neglect of the batter would have minimal effect), using soil data provided by Shell. Winkler spring elements representing skin friction (t-z springs), end bearing (Q-z springs) and lateral resistance (p-y springs) were generated for the static pile-soil model in accordance with API RP 2A Section 6 (API, 1993). The model was then used to generate relationships for vertical (pullout) load vs. vertical (pullout) deflection, vertical (plunging) load vs. vertical (plunging) deflection, lateral load vs. lateral deflection, and moment about the horizontal vs. lateral deflection (Figure 2.2.3-5). No attempt was made to model torsional response, and no attempt was made to couple the lateral deflection and rotation about the horizontal. While the neglect of these effects might cause minor errors in the displacement of the structure, it was felt they would not significantly influence the collapse load, unless the foundation was truly the weak link (which from historical experience is believed not to be the case).

The spring-to-ground element was oriented to the axis of the pile to account for batter (Figure 2.2.3-6). It should be noted that after the first few trial analyses

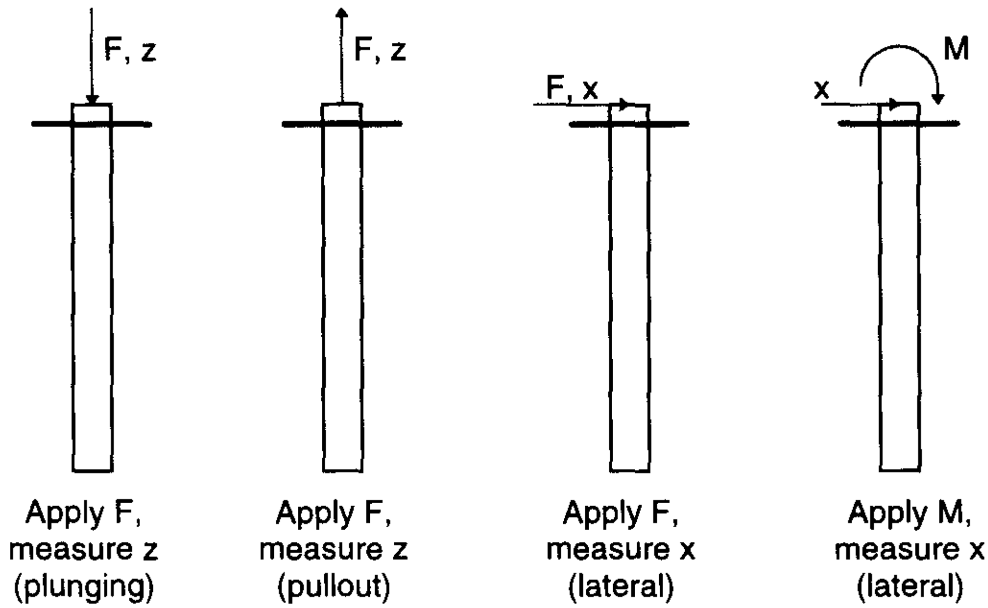

Figure 2.2.3-5: Force-Displacement Relations for Spring-to-Ground Elements

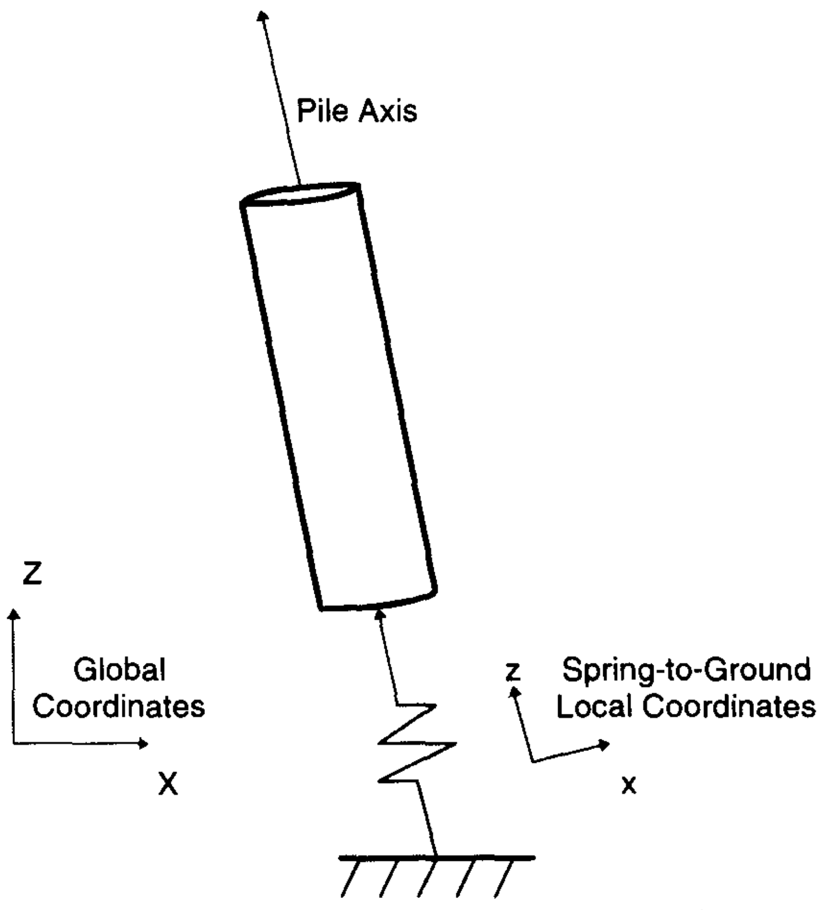

Figure 2.2.3-6: Spring-to-Ground Element Local Orientation

using these foundation springs, results indicated that the foundation was failing both axially and laterally. Hence, the strengths of the foundation spring models were increased to prevent foundation failure; this issue is discussed further in Section 2.2.5 of this report.

2.2.4 Loads Applied to Platform

Information used to develop the loads on the platform came from several sources. Shell supplied information on deck dead loads and operating equipment loads, as well as projected areas for use in calculating wind and wave loads on the decks and boat landings. API RP 2A Section 17 (API, 1994) guidelines were used to develop an appropriate set of environmental loads. With the initial selection of surge/tide, current profile and wind speed profile, the wave height was adjusted until the load factor for all environmental loads was unity at the point of failure.

Based on results from oceanographic studies (Bea, 1975) storm surge and tide were selected as 3 ft. Current was evaluated to be 2.3 knots, with a profile which was constant to a depth of -200 ft, varied linearly from 2.3 to 0.2 knots from -200 ft to -300 ft, and then remained constant at 0.2 knots to the mudline. Wind speed was evaluated to be 100 mph for the +33 ft MGL, and at 130 mph for the +130 ft MGL (1-minute gust velocities). The period of the storm wave was evaluated to be 13.5 sec, and Stoke's V-order wave theory was selected to establish the wave kinematics. In all cases, the wind and current were considered to be acting in the same direction as and concurrently with the wave.

Hydrodynamic coefficients were chosen based on recent studies and API guidelines. A wave kinematics factor of 0.88 was used for both the deck and jacket loads. Current blockage factors of 0.80 for broadside loads and 0.70 for end-on loads were also used. For deck wave loads, the drag coefficient C_D was chosen to be 2.5 (heavily equipped/cluttered deck). For the boat landings, C_D was chosen to be 1.2 (rough cylindrical members). 1.5 inches marine growth was assumed from 0 ft MGL to a depth of -150 ft MGL. For cylindrical members, the drag coefficient C_D was chosen as 0.63 for smooth members, and 1.2 for rough members; the inertia coefficient C_M selected was 1.5 (Rodenbusch, Kallstrom, 1986; Tromans, van de Graaf, 1992).

2.2.5 Analysis Cases

The platform was analyzed for three principal wave attack directions: end-on (north-traveling wave), and broadside (east- and west-traveling waves). As the piles were not expected to be the weak link, wave attack cases off the principal axes were neglected. Both broadside cases were considered as the framing to resist load in each of those directions is not anti-symmetric, as it is for the case of end-on loads. However, it should be noted that extreme waves from the west are not expected due to the location of the structure.

In addition to varying the direction of wave attack, several different foundation fixity conditions were used. In the first set of analyses, the piles were fixed at the mudline. The results of these analyses were expected to give good estimates of both the collapse load and the failure mode (assuming failure occurred in the jacket or deck legs), and to allow the wave height which loaded the structure to collapse with a load factor of unity to be finalized. In the second and third sets of analyses, non-linear spring-to-ground elements capturing the behavior of the imbedded portions of the piles were used to represent foundation behavior; these were derived as described in the discussion of platform modeling. The second set analyses utilized spring-to-ground elements which were derived from the detailed pile-soil model. However, after the first few trial analyses, it was found the piles were failing both in the axial and lateral directions. To counteract this, the strengths of the spring-to-ground elements were factored up by 1.5 to recognize the site soil sampling, testing, and dynamic-cyclic loading effects; SP62A was not expected to experience foundation failure based on historical data (Bea, 1975; Marshall, Bea, 1976; Tromans, van de Graaf, 1992). Force-displacement relations for the unmodified and factored foundation springs are summarized in Section 3.1. The third set of analyses make use of these factored foundation springs; the results of this third set are presented below as best characterizing the platform's ULS.

2.2.5.1 End-On Wave Attack:

For the case of end-on wave attack (north-traveling wave), the wave height was adjusted until collapse of the structure occurred at a load factor of 1.05. This was achieved for an 80 ft wave, with the crest location just north of the platform's midsection. The load profile on the platform for this case may be seen in Figure 2.2.5.1-1. ULS was reached for a lateral load of 7440 kips. A plot of base shear vs. cellar deck displacement may be seen in Figure 2.2.5.1-2. Collapse occurred following the failure in compression of diagonal brace A3-A4 in the fourth jacket bay; this was quickly followed by the failure of the remaining compression braces in jacket bays three and four (frames A and B). Plots of critical brace axial force vs. cellar deck displacement may be seen in Figure 2.2.5.1-3. It should be noted that the solution indicated minor yielding in some members before the failure of the first brace; however, it questionable as to whether any of this damage could have been ascertained during an inspection. Further, because of the rigidity of the skirt piles relative to the main piles, indications of minor yielding in some of the horizontal and vertical framing was given as the main piles and jacket legs tended to deflect laterally more than the skirt piles and their guides. The structure exhibited extremely brittle behavior, having no reserve strength after the failure of the first brace. However, the platform still possessed approximately 75% residual strength; this was accounted for by the

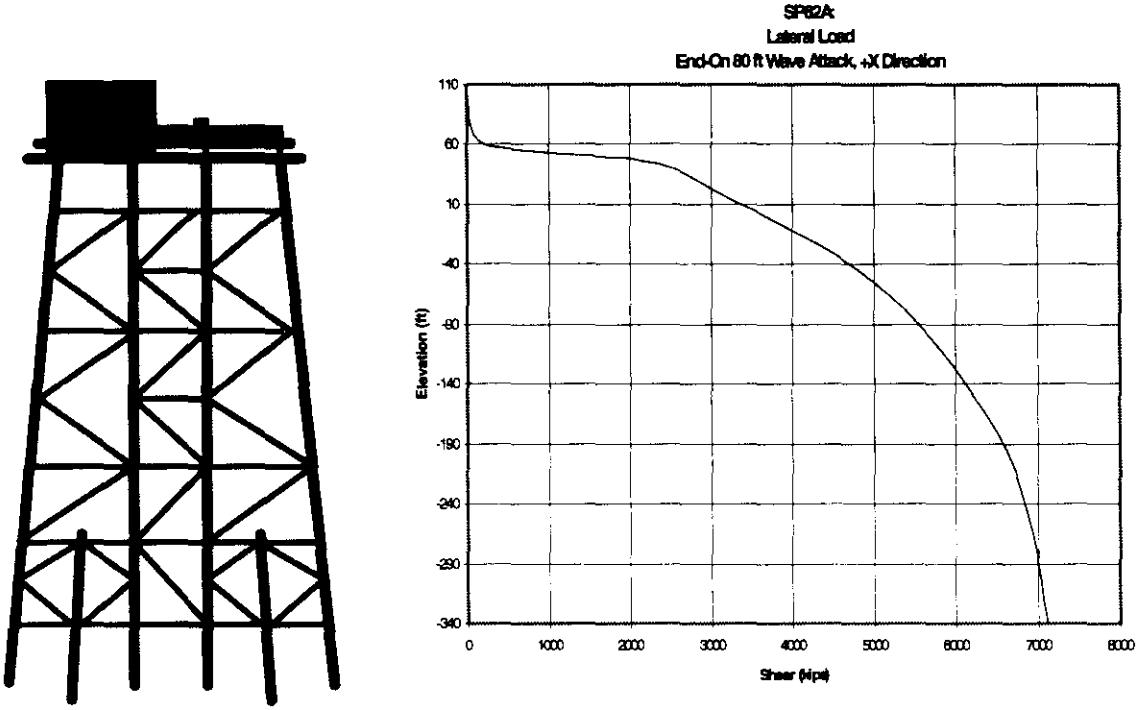

Figure 2.2.5.1-1: Storm Shear Profile
80 ft End-On Wave Attack (North Traveling)

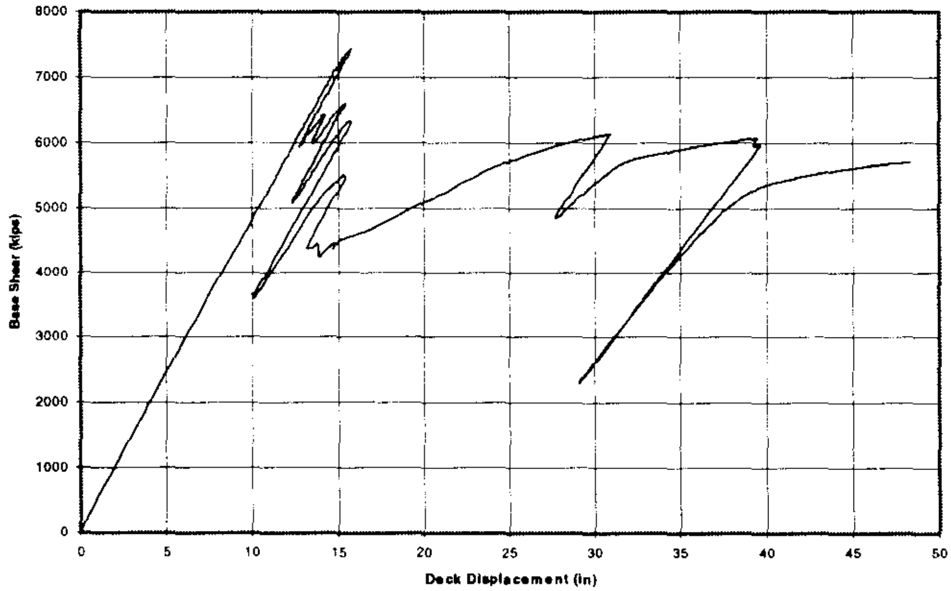

Figure 2.2.5.1-2: Base Shear vs. Cellar Deck Displacement
80 ft End-On Wave Attack (North Traveling)

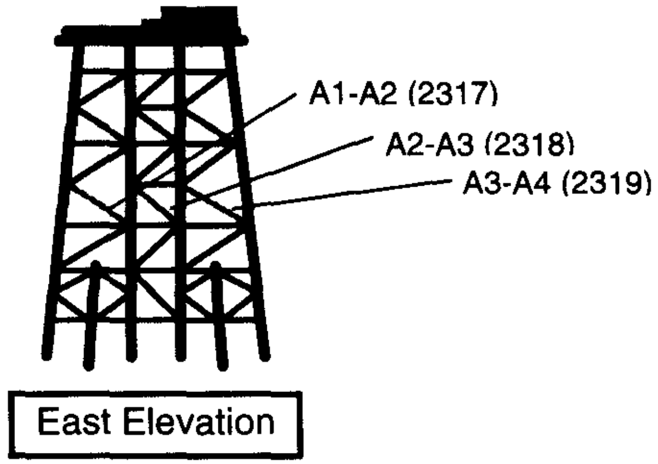

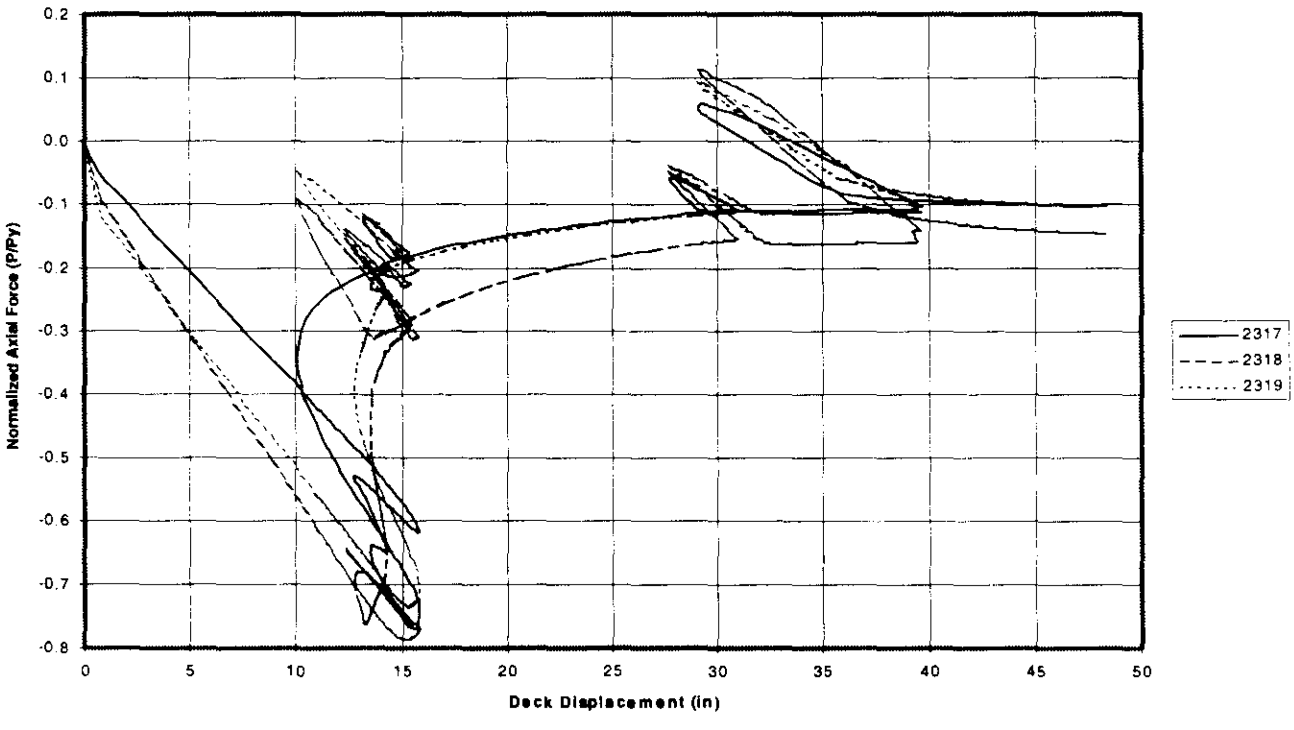

Figure 2.2.5.1-3: 4th Jacket Bay (Frame A) Braces Axial Force vs. Cellar Deck Displacement 80 ft End-On Wave (North Traveling)

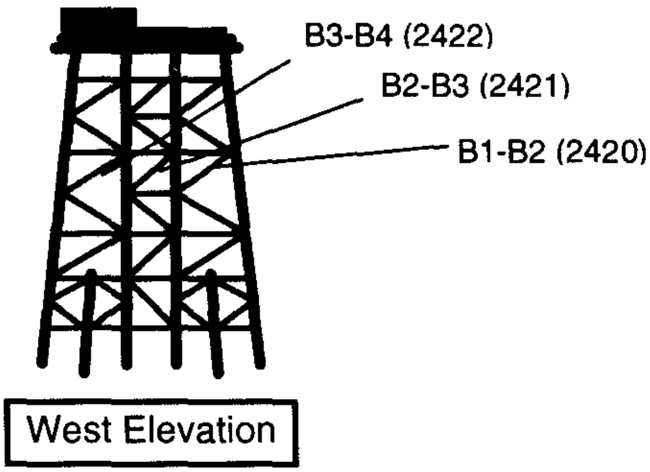

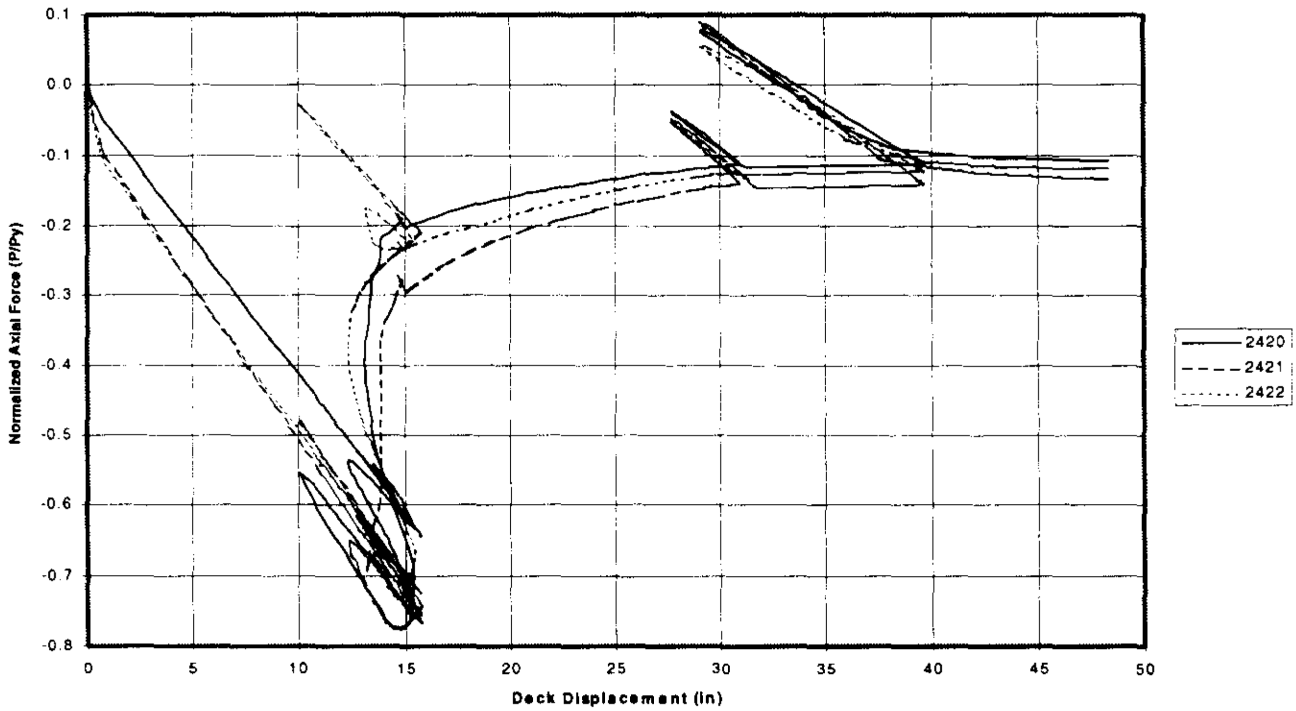

Figure 2.2.5.1-4: 3rd Jacket Bay (Frame B) Braces Axial Force vs. Cellar Deck Displacement 80 ft End-On Wave (North Traveling)

yielding of the jacket legs and main piles and the action of the tension braces in the third and fourth jacket bays.

2.2.5.2 Broadside Wave Attack:

For the case of broadside wave attack, cases were run for both a west-traveling and an east-traveling wave, as the framing which resists loads in each direction is different. In both cases, it was found that an 84 ft wave loaded the structure to its ULS, with the crest located at the midsection of the platform. The load profile associated with this wave is shown in Figure 2.2.5.2-1.

For the west-traveling wave, collapse occurred at a load factor of 1.11, giving a total lateral load of 9510 kips. Collapse for the west-traveling wave attack case was initiated by the failure of diagonal brace A1-B1 in the second jacket bay, followed by the yielding of the tension braces in the same bay (frames 2,3,4). Plots of base shear vs. cellar deck displacement and critical brace axial force vs. deck displacement may be seen in Figures 2.2.5.2-2 and 2.2.5.2-3. Examining the plot of base shear vs. deck displacement, it is easy to see the structure exhibits less-pronounced brittle behavior, but residual strength is quite high, on the order of 80% (following the failure of additional braces in the jacket when the cellar deck displacement is near 55 in.).

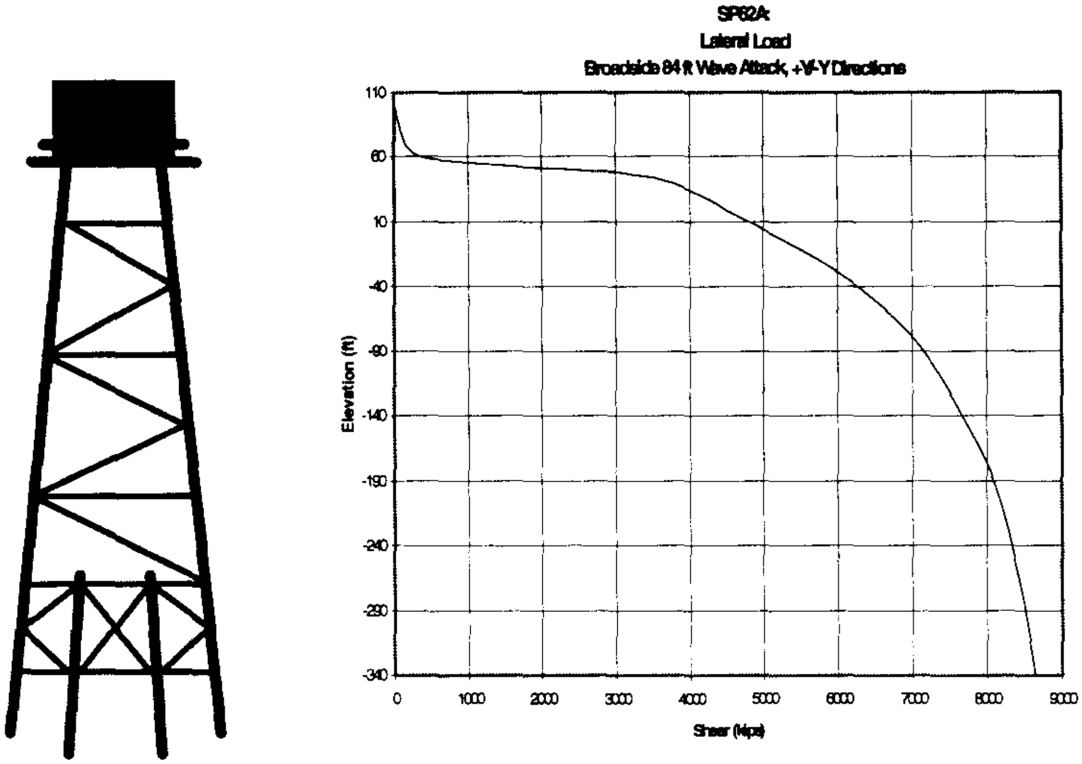

Figure 2.2.5.2-1: Storm Shear Profile for Broadside Loads

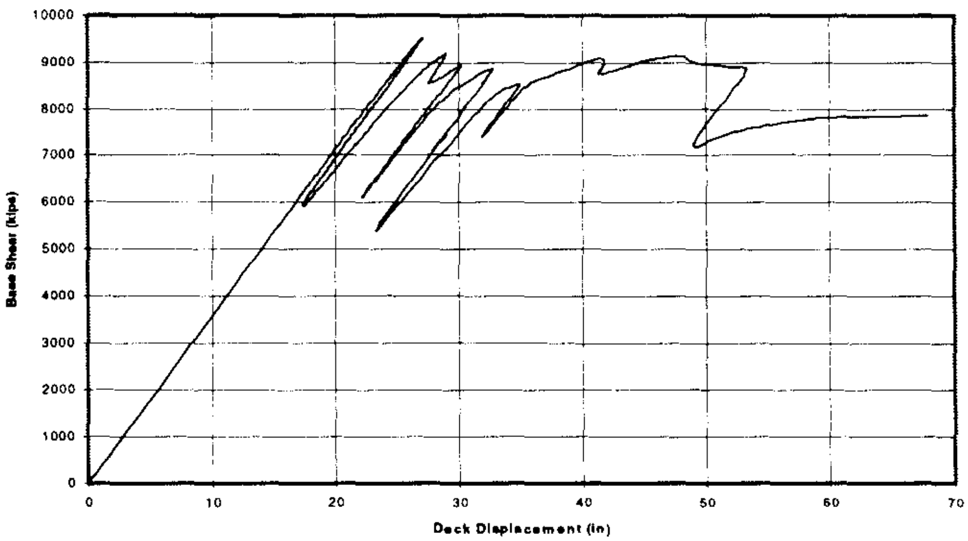

Figure 2.2.5.2-2: Base Shear vs. Cellar Deck Displacement
84 ft Broadside Wave Attack (West Traveling)

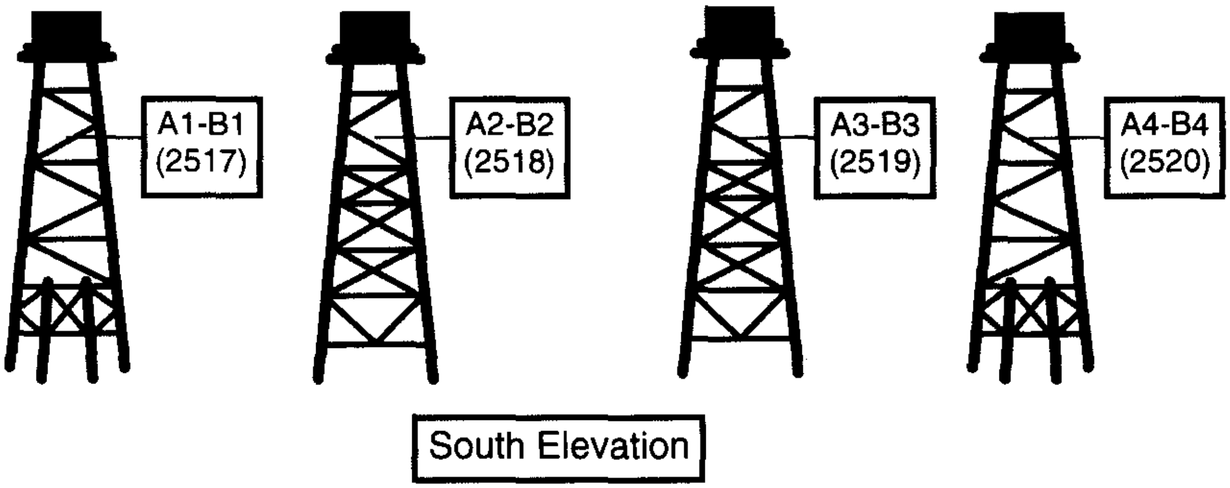

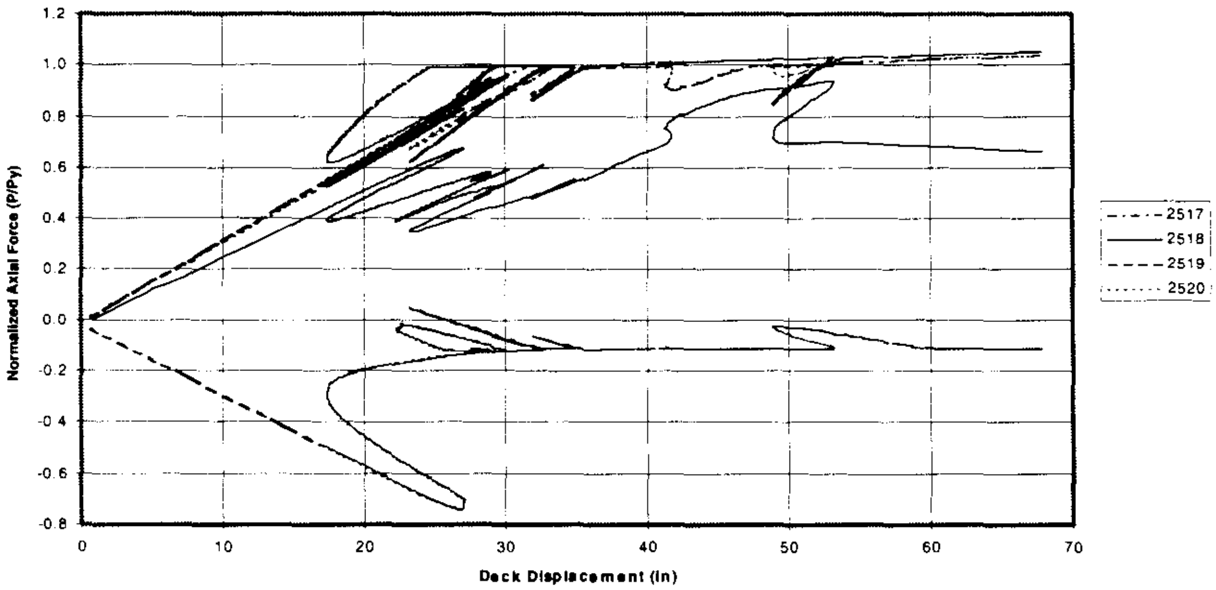

Figure 2.2.5.2-3: Second Jacket Bay (Frames 1-4) Braces Axial Force vs. Cellar Deck Displacement 84 ft Broadside Wave (West Traveling)

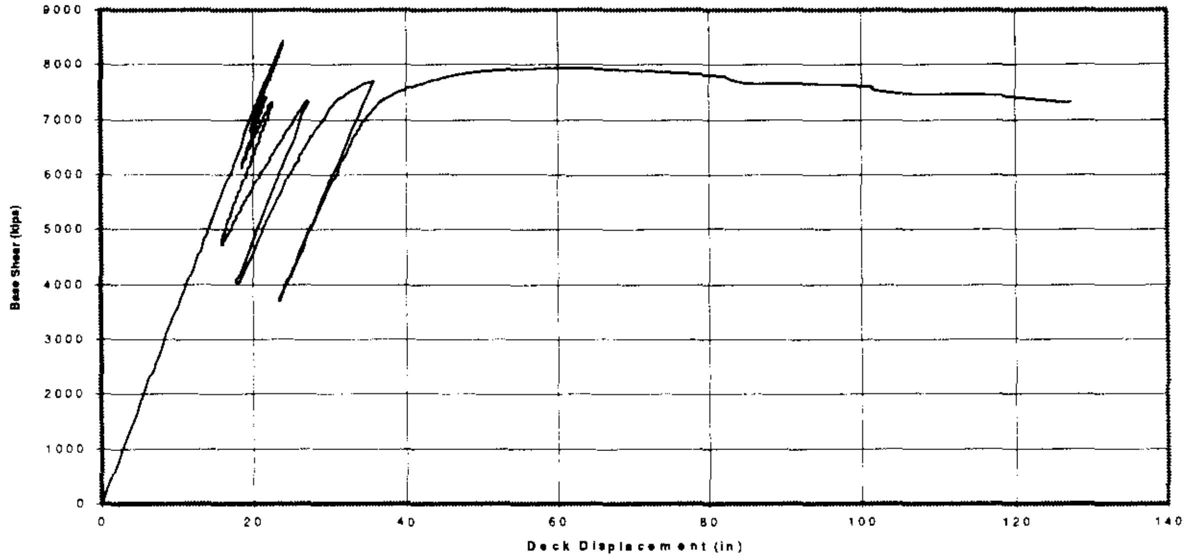

Figure 2.2.5.2-4: Base Shear vs. Cellar Deck Displacement
84 ft Wave Attack (East Traveling)

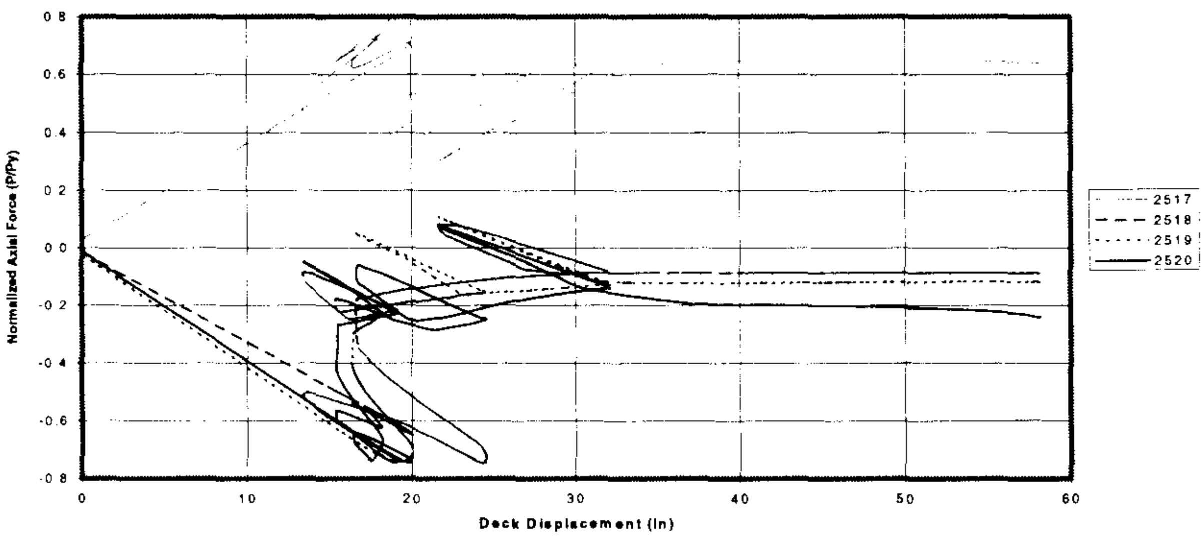

Figure 2.2.5.2-5: Second Jacket Bay (Frames 1-4) Braces
Axial Force vs. Cellar Deck Displacement
84 ft Broadside Wave (East Traveling)

For the case of an east-traveling wave, failure was initiated by failure of diagonal braces A2-B2, A3-B3 and A4-B4 in the second jacket bay; this was followed by the yielding of the tension brace in the same bay (A1-B1). Collapse occurred for a load factor of 0.98, giving a total lateral load of 8430 kips. Plots of base shear vs. cellar deck displacement and critical brace axial force vs. deck displacement may be seen in Figures 2.2.5.2-4 and 2.2.5.2-5. For this direction of wave attack, the structure exhibited nearly elastic-plastic behavior, with the collapse load being reached upon the failure of the first member. Residual strength amounted to approximately 90% of the collapse load.

2.2.6 Comparison with Observed Performance

As noted in Section 2.2.2, SP62A and two sister platforms were subjected to extreme environmental loads well in excess of original design loads when Hurricane Camille passed through the region in 1969. The total maximum lateral loadings developed during Camille are estimated to be in the range of 6000 to 6700 kips. Based of the results of the ULS evaluation, it is apparent that SP62A would likely have survived Camille with little or no noticeable damage. As a point of interest, this ULS analysis indicates the platform's static lateral loading strength is 7440 kips (end-on loading). The original design load was 3300 kips (Marshall, Bea, 1976).

Tromans and van de Graaf (1992) obtained an end-on loading capacity of 8,500 kips. This capacity did not include wave-in-the-deck loadings. Based on Tromans and van de Graaf's overload ratio that accounted for deck wave loadings, an end-on loading capacity of 7230 kips was estimated. This is in good agreement with the results obtained in this study. Tromans and van de Graaf estimated that the total maximum lateral loading developed during Camille was approximately 6100 kips.

The dynamic loading - nonlinear response characteristics of SP62A have been studied by Bea and Young (1993). This study resulted in an expected (best estimate) dynamic nonlinear loading capacity factor of $F_v = 1.2$ for this platform. These results indicate that the platform could be expected to have an ultimate dynamic lateral loading capacity of about 8930 kips.

Of further interest, however, is the case of SP62B; this platform survived a large end-on wave with minor structural damage to the deck, and with no noticeable damage in the jacket. Given the results of the ULS evaluation indicate an extremely brittle failure mode for this loading situation, it would be expected that there could have been some minor yielding within the jacket which would only be noticeable at a very close, detailed inspection. Thus, the results of the ULS can be said to be in good agreement with the performance of these structures.

It should be remembered that earlier trial analyses indicated significant foundation displacements or failure would have occurred. Similar results were obtained by Tromans and van de Graaf (1992). No foundation damage was observed on any of the three South Pass 62 platforms. Hence, using traditional API based static pile stiffness and capacity characterizations intended for use in design can result in significant underestimates of the pile foundation capacities and stiffnesses.

2.3 <u>Ship Shoal 274A</u>

2.3.1 Platform Characteristics

SS274A was installed in the Ship Shoal region of the Gulf of Mexico off Louisiana in 1964. The platform is an 8-leg jacket structure sited in 213 ft of water (see Figure 2.3.1-1). It is an unmanned self-contained drilling and production platform, and it supports 12 24 inch-diameter conductors. The platform was originally designed in 1963 for a 55 ft wave with no current, and Morison drag and inertia force coefficients of 0.5 and 1.5, respectively (van de Graaf, Tromans, 1991). Wave forces on barge bumpers, boat landings and other appurtenances were neglected in the platform design; the original design lateral load for the platform was 1890 kips (Lee, 1988).

SS274A has decks at +43 ft and +57 ft MGL (mean Gulf level). The base dimensions of the jacket are 171.75 ft x 91.75 ft. The perimeter framing of the jacket is battered to 1:10. The jacket legs are fabricated from sections 46 inches

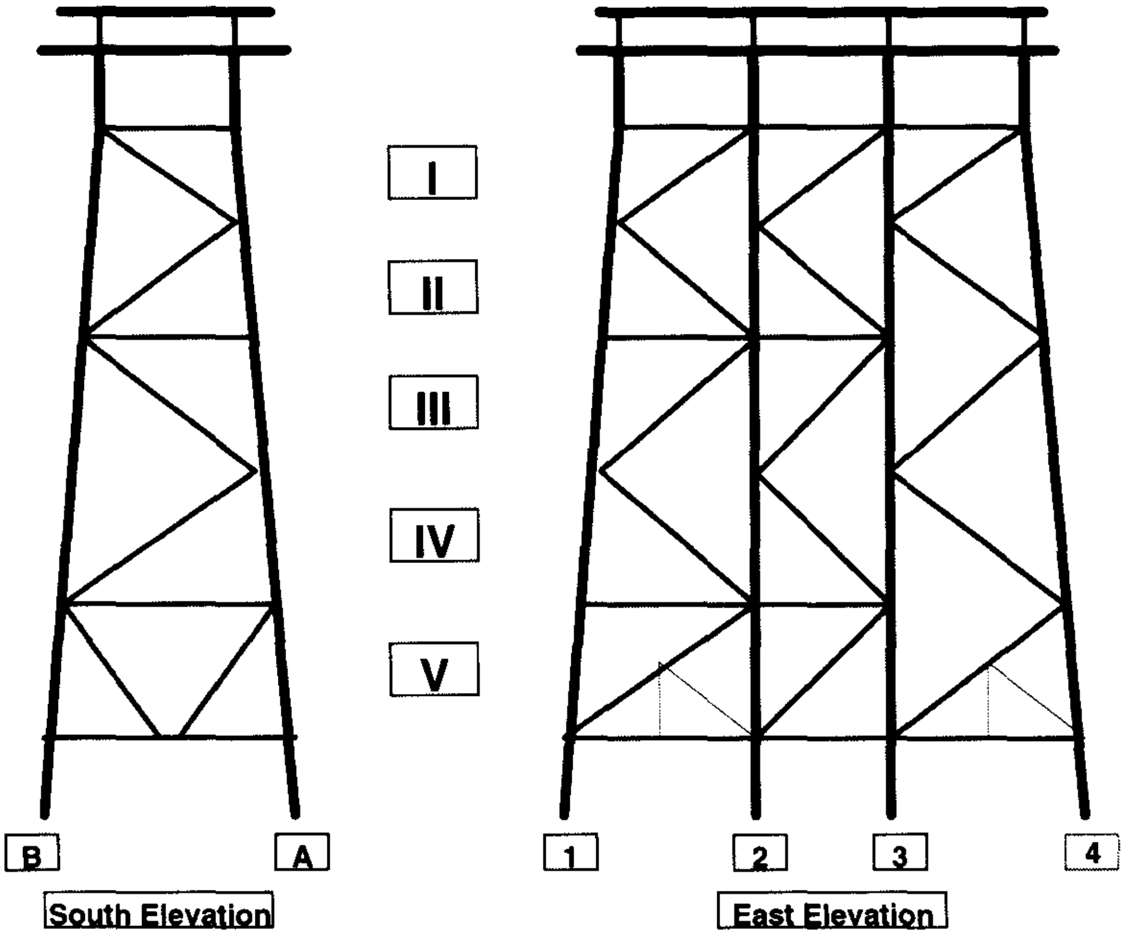

Figure 2.3.1-1: Ship Shoal 274 A Platform Elevations

in diameter (w.t. 0.5 inch, w.t. 1.0 inch for launch truss sections in legs 2 and 3). Braces in the jacket range from 26 inches in diameter (w.t. 0.5 inch) in the fourth jacket bay to 16 inches in diameter (w.t. 0.5 inch) in the top bay. The major joints in the jacket are canned, with the cans having w.t. 1.0 inch.

The foundation consists of 8 piles driven through the jacket legs. The piles are 42 inches in diameter (w.t. from 0.625 inch to 1.125 inches); they pass through the legs and are welded off at +12.5 ft MGL. The deck legs are 36 inches in diameter (w.t. 0.5 inch) and are welded to the tops of the piles. All piles were designed to have 285 ft penetration. However due to insufficient pile driver energies, most were driven to little more than 250 ft penetration. Information on the soil conditions was provided by Shell. Based on on-site soil borings, the soil profile has been characterized as:

0-38.5	ft	soft clay
38.5-58	ft	silty sand, fine sand
58-278	ft	stiff clay, flocculated below 140 ft
278+	ft	dense sand

It should be noted that because the piles were underdriven, they are not founded on the sand layer at 278 ft.

The deck legs, jacket members and the piles are made primarily from A36 steel. The strength of the A36 material has been taken to be 43 ksi, using the same evaluations concerning material behavior that were used for SP62A.

2.3.2 Platform History

In 1964, Hurricane Hilda passed over the Ship Shoal region, subjecting SS274A and nearby structures to very severe wind and wave loads (Bea, 1975). Inferences from miscellaneous damage indicate that SS274A was struck by a wave or waves in the range of 53-57 ft-high; it is unclear as to whether or not the wave actually entered the lower deck (Bea, 1975; Lee, 1988). Nevertheless, this is extremely close to the design wave height. The principal direction of the wave attack is believed to have been from the southeast, but this is unclear (Lee, 1988). Given the multi-directional properties of the waves close to the center of this storm, large waves could be expected to develop from wind waves from the east superimposed on swell from the south.

The platform sustained moderate damage as a result of this loading; the damage and date of discovery is listed below:

1964	Crack in first bay diagonal B3-A3 between corrosion wrap and horizontal. Crack in first bay diagonal B3-B2 between gussets and corrosion wrap.

1970 Parted bulge in leg A1 at -10 MGL. Buckled section in leg A3 at -10 MGL. Crack in first bay diagonal B2-B1 above corrosion wrap.

The damage to B3-A3 was found immediately after Hilda. The damage to B3-B2 was found three months later. The damage discovered in 1970 was found during an underwater inspection of the platform. It should be mentioned that other damage has been located since 1970, including several bent members (first bay diagonals B2-A2, A2-A3); however, it is unclear as to whether this damage occurred during Hilda or was the result of accidents or operations (Lee, 1988). The damage to the platform identified during this series of inspections has been repaired. The platform is in service today.

2.3.3 Structural Model of Platform

The analytical model developed for SS274A contains the major structural components of the platform (Figures 2.3.3-1,2,3). It was assumed the deck members would not fail; hence only the main framing members of the deck were included. Inelastic deformation of the deck members was suppressed. The conductor framing was included in the model, but the conductors themselves were modeled as four sets of "equivalent" conductors, with a diameter sized such that the Morison drag load generated on each equivalent set would be equal to the load generated on three of the original conductors. The conductor elements were

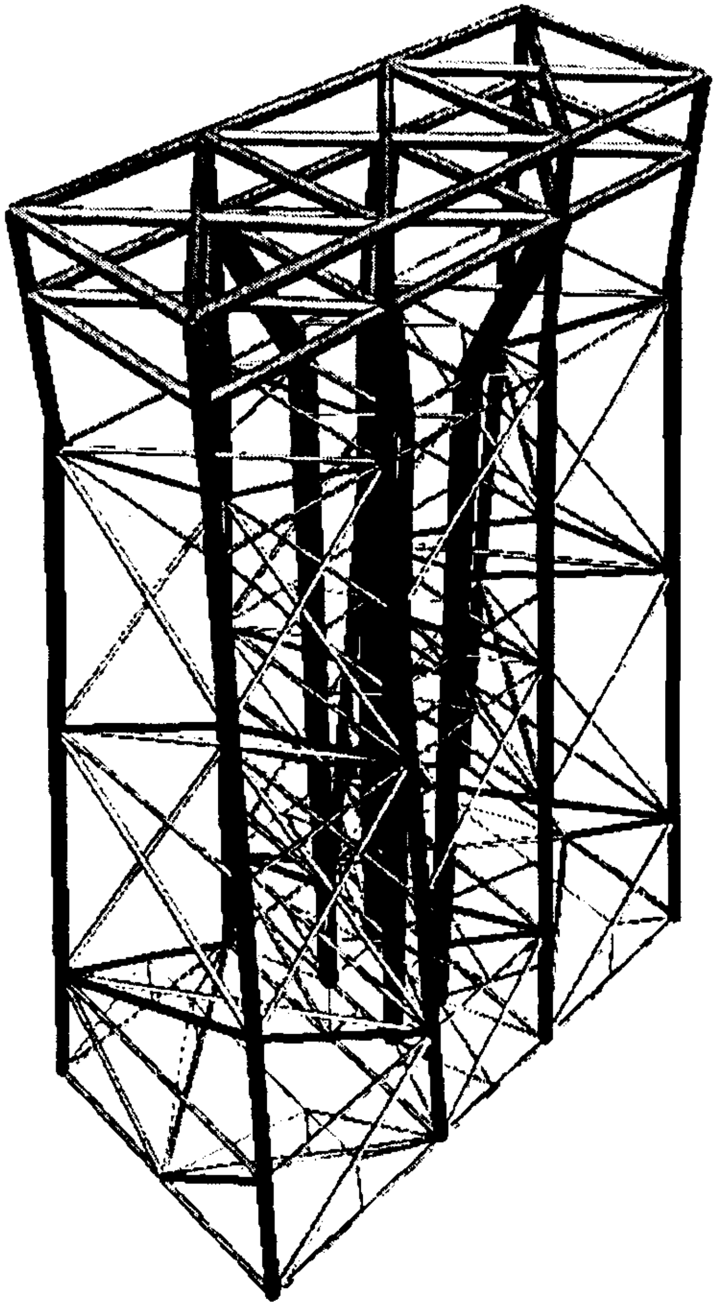

Figure 2.3.3-1: Ship Shoal 274 Platform Isometric

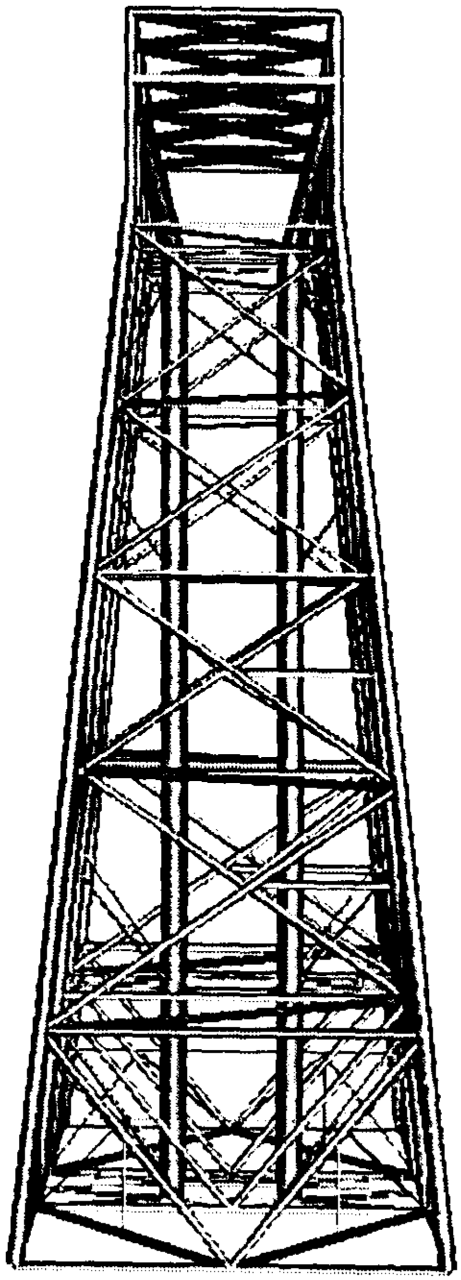

Figure 2.3.3-2: Ship Shoal 274 Platform South Elevation

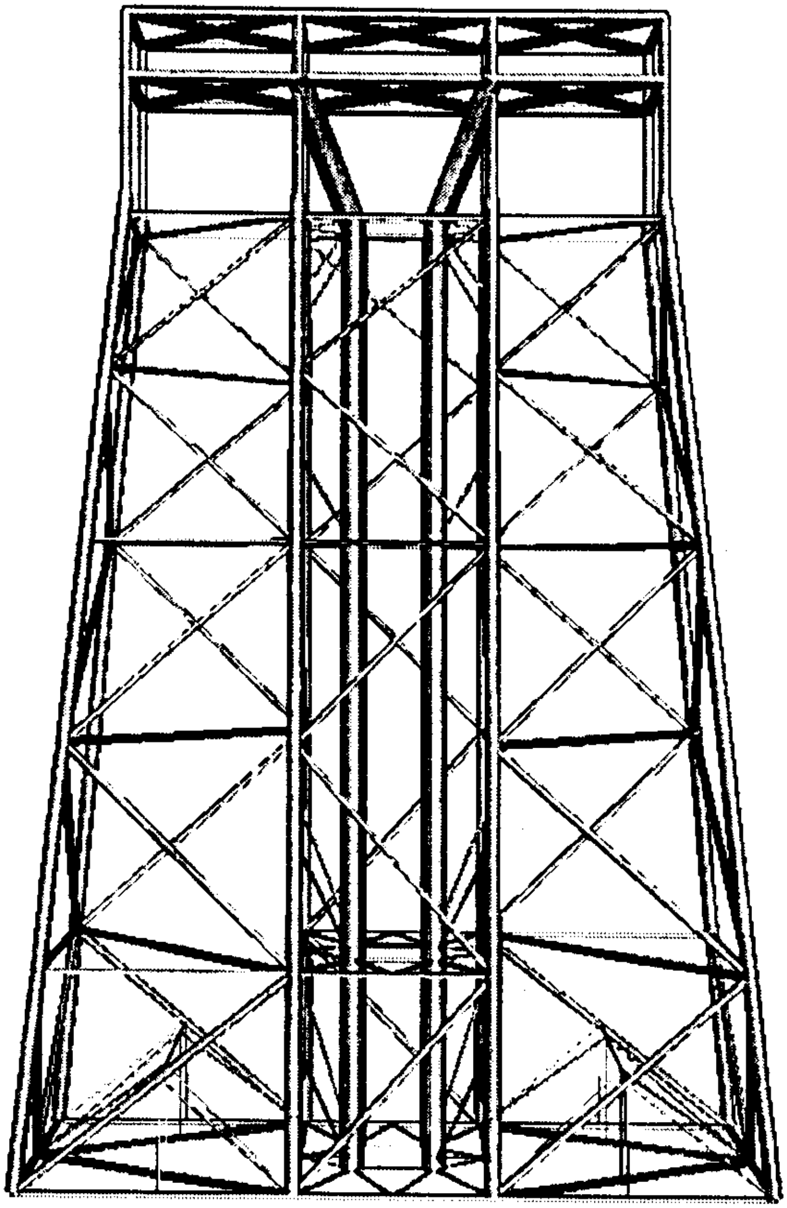

Figure 2.3.3-3: Ship Shoal 274 Platform East Elevation

declared non-structural elements so as not to contribute to the global stiffness of the platform.

Brace elements in the jacket were given a single curvature imperfection equal to 0.0015L, with deformation conservatively assigned in the direction of the load. Imperfections were only assigned to elements for a specific load case if those elements were identified as being part of the failure mode from an initial "trial" analysis in which no imperfections were assigned.

The analysis was performed assuming rigid joints. The platform joints are comprised of heavy wall chord and branch cans. Evaluation of joint capacities and stiffnesses indicated that the assumption of rigid joints was valid.

The main piles above the mudline were modeled discretely from the jacket sleeves, with the two constrained together for the purposes of lateral displacement. To capture the behavior of the piles below the mudline, the same approach was used as for the analysis of SP62A (see Section 2.2.3), using soil data provided by Shell. It should be noted that after the first few trial analyses using these foundation springs, results indicated that the foundation was failing laterally; lateral displacements at the mudline was excessive. Hence, the strengths and stiffnesses of the foundation spring models were increased to recognize the effects of site soil sampling, testing, and dynamic - cyclic loading effects. This issue is discussed further in Section 2.3.5 of this report.

2.3.4 Loads Applied to Platform

Information used to develop the loads on the platform came from several sources. Shell supplied information on deck dead loads and operating equipment loads, as well as projected areas for use in calculating wind and wave loads on the decks and boat landings. API RP 2A Section 17 (API, 1994) guidelines were used to develop an appropriate set of environmental loads. With the initial selection of surge/tide, current profile and wind speed profile, the wave height was adjusted until the load factor for all environmental loads was unity at the point of failure.

Based on results from oceanographic studies, surge/tide was selected as 3 ft. Current was estimated to be 2.3 knots, with a profile which was constant to a depth of -200 ft, varied linearly from 2.3 to 0.2 knots from -200 ft to -300 ft (cutoff at the mudline, -213 ft). Average wind speed was estimated to be 125 mph for the decks (1-minute gust velocities). The period of the storm wave was estimated to be 13.5 sec, and Stoke's V-order wave theory was selected to establish the wave kinematics. In all cases, the current and wind were considered to be acting in the same direction and at the same time as the wave.

Hydrodynamic coefficients were chosen based on recent studies and API guidelines. A wave kinematics factor of 0.88 was used for both the deck and jacket loads. Current blockage factors of 0.80 for broadside loads and 0.70 for end-on loads were also used. For deck wave loads, the drag coefficient C_D was chosen to be 2.5 (heavily equipped/cluttered deck). For the boat landings, C_D was chosen to be 1.2 (rough cylindrical members). 1.5 inches marine growth was assumed from 0 ft MGL to a depth of -150 ft MGL. For cylindrical members, the drag coefficient C_D was chosen as 0.63 for smooth members, and 1.2 for rough members; the inertia coefficient C_M selected was 1.5 (Rodenbusch, Kallstrom, 1986; van de Graaf, Tromans, 1991; Tromans, van de Graaf, 1992).

2.3.5 Analysis Cases

The platform was analyzed for two principal wave attack directions: end-on (north-traveling wave), and broadside (west-traveling wave). As the piles were not expected to be the weak link, wave attack cases off the principle axes were neglected.

In addition to varying the direction of wave attack, several different foundation fixity conditions were used. In the first set of analyses, the piles were fixed at the mudline. The results of these analyses were expected to give good estimates of both the collapse load and the failure mode (assuming failure occurred in the jacket or deck legs), and to allow the wave height which loaded the structure to collapse with a load factor of unity to be finalized. In the second and third sets of analyses, non-linear spring-to-ground elements capturing the behavior of the imbedded portions of the piles were used to represent foundation behavior; these were derived as described in the discussion on platform modeling. The second set analyses utilized spring-to-ground elements which were derived from the detailed pile-soil model based on static pile-soil interaction characterizations. However, after the first few trial analyses, it was found the piles were failing both in the axial and lateral directions.

To counteract this, the lateral strengths of the spring-to-ground elements were factored up by 1.5 to recognize site soil sampling, testing, and dynamic-cyclic loading effects. The lateral stiffnesses of the springs were increased by a factor of 4 to recognize the foregoing soil - pile interaction effects. Platform inspections following Hilda did not disclose the presence of any significant foundation deformations. Force-displacement relations for the unmodified and factored foundation springs are summarized in Section 3.1. The third set of analyses make use of these factored foundation springs; the results of this third set are presented below as best characterizing the platform's ULS.

2.3.5.1 End-On Wave Attack:

For the case of end-on wave attack (north-traveling wave), the wave height was adjusted until collapse of the structure occurred at a load factor of 0.957. This was achieved for a 67 ft wave, with the crest location just north of the platform's midsection. The load profile on the platform for this case may be seen in Figure 2.3.5.1-1. ULS was reached for a lateral load of 4570 kips. A plot of base shear vs. cellar deck displacement may be seen in Figure 2.3.5.1-2. Collapse occurs following the failure in compression of diagonal brace B3-B4 in the third jacket bay; this was quickly followed by the failure of the remaining compression braces in jacket bays three and four (frames A and B). Plots of critical brace axial force vs. cellar deck displacement may be seen in Figure 2.3.5.1-3. The structure exhibits extremely brittle behavior, having no reserve strength after the failure of the first brace.

2.3.5.2 Broadside Wave Attack:

For the case of broadside wave attack (west-traveling wave), the wave height was adjusted until collapse of the structure occurred at a load factor of 0.99. This was achieved for a 67 ft wave, with the crest location at the platform's midsection. The load profile on the platform for this case may be seen in Figure 2.3.5.2-1. ULS was reached for a lateral load of 5250 kips. A plot of base shear vs. cellar deck displacement may be seen in Figure 2.3.5.2-2. The collapse mechanism involves several members. The first member to fail is diagonal brace A4-B4 in the third jacket bay; this member fails in compression. This failure is followed by the failures of diagonal braces A2-B2 (first jacket bay) and A3-B3 (second jacket bay), both in compression. It should be noticed there is a slight amount of reserve strength following the failure of A4-B4. Plots of critical brace axial force vs. cellar deck displacement may be seen in Figure 2.3.5.2-3. It

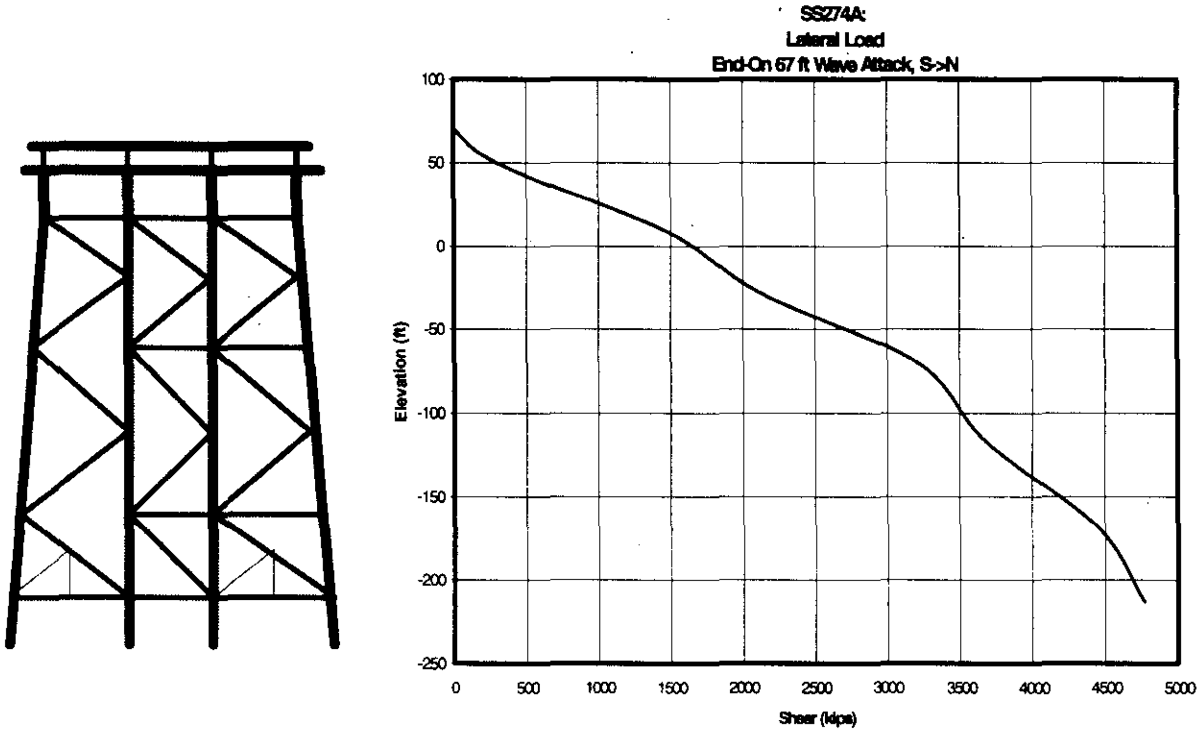

Figure 2.3.5.1-1: Storm Shear Profile for End-On Load

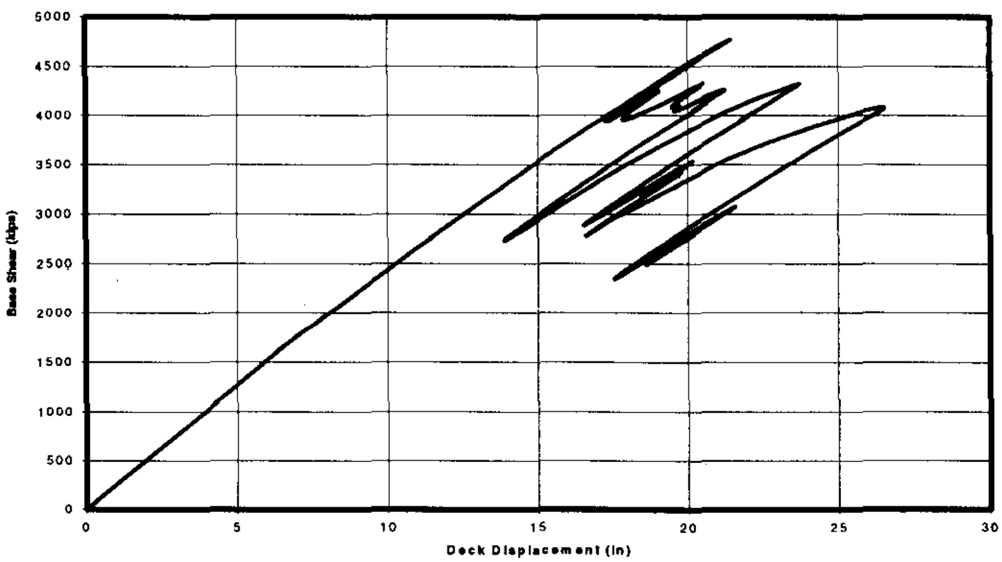

Figure 2.3.5.1-2: Base Shear vs. Cellar Deck Displacement
67 ft End-On Wave Attack (North Traveling)

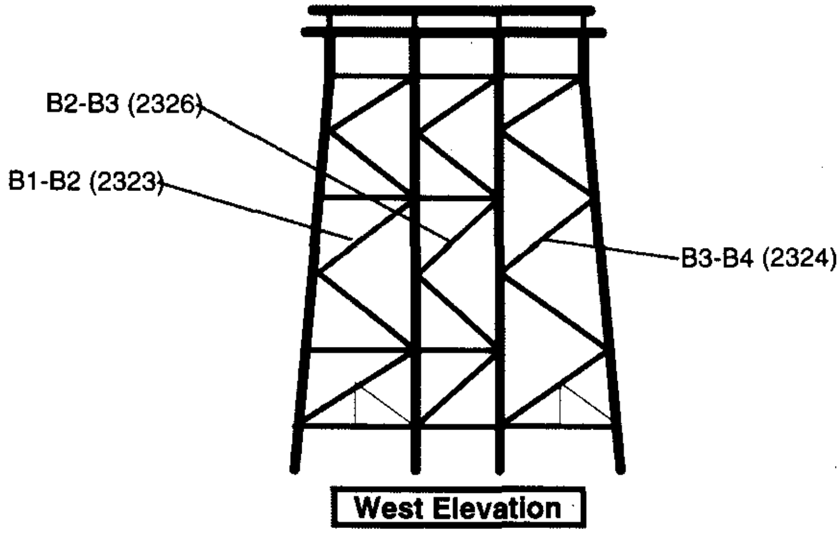

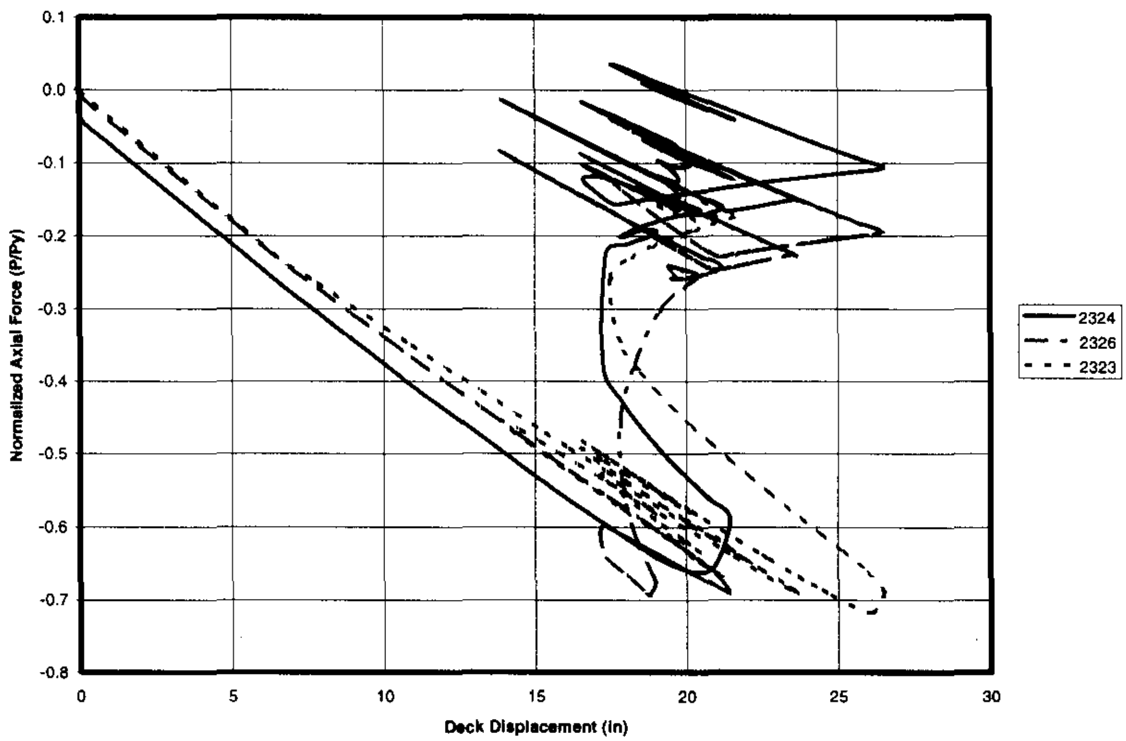

Figure 2.3.5.1-3: 3rd Jacket Bay (Frame B) Braces Axial Force vs. Cellar Deck Displacement 67 ft End-On Wave (North Traveling)

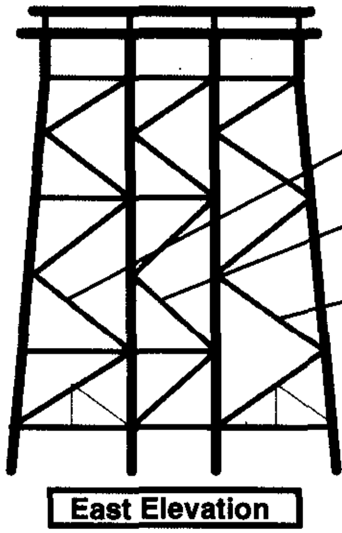

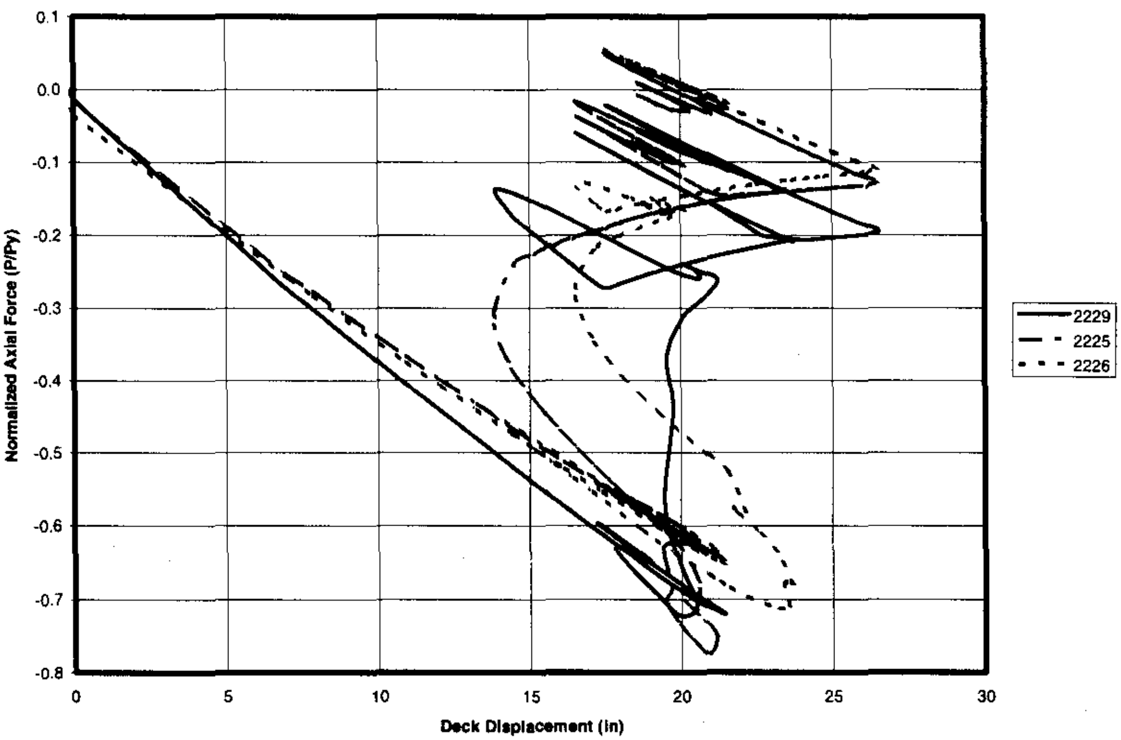

Figure 2.3.5.1-4: 4th Jacket Bay (Frame A) Braces Axial Force vs. Cellar Deck Displacement 67 ft End-On Wave (North Traveling)

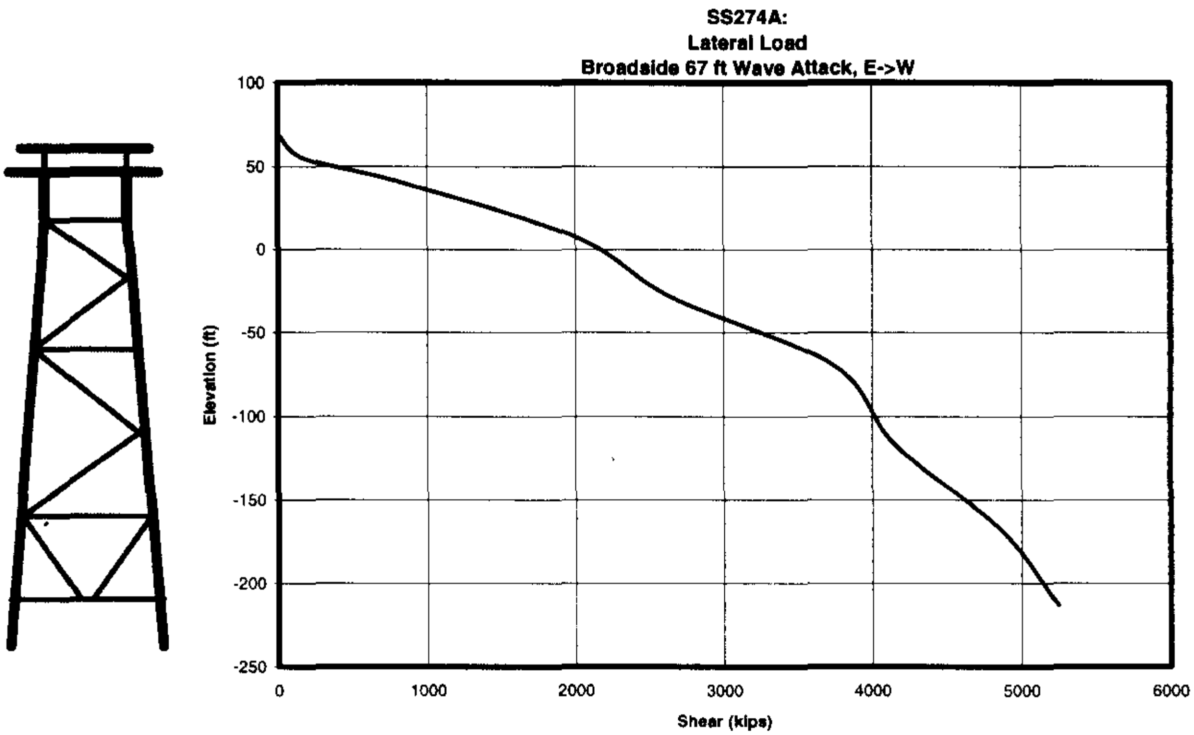

Figure 2.3.5.2-1: Storm Shear Profile for Broadside Load

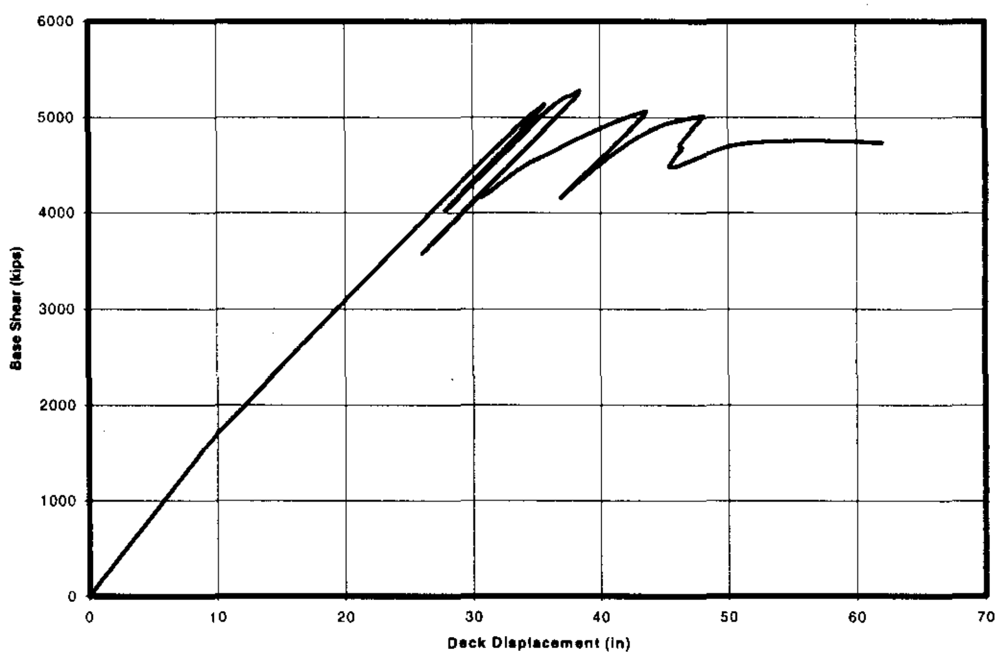

Figure 2.3.5.2-2: Base Shear vs. Cellar Deck Displacement 67 ft Broadside Wave Attack (West Traveling)

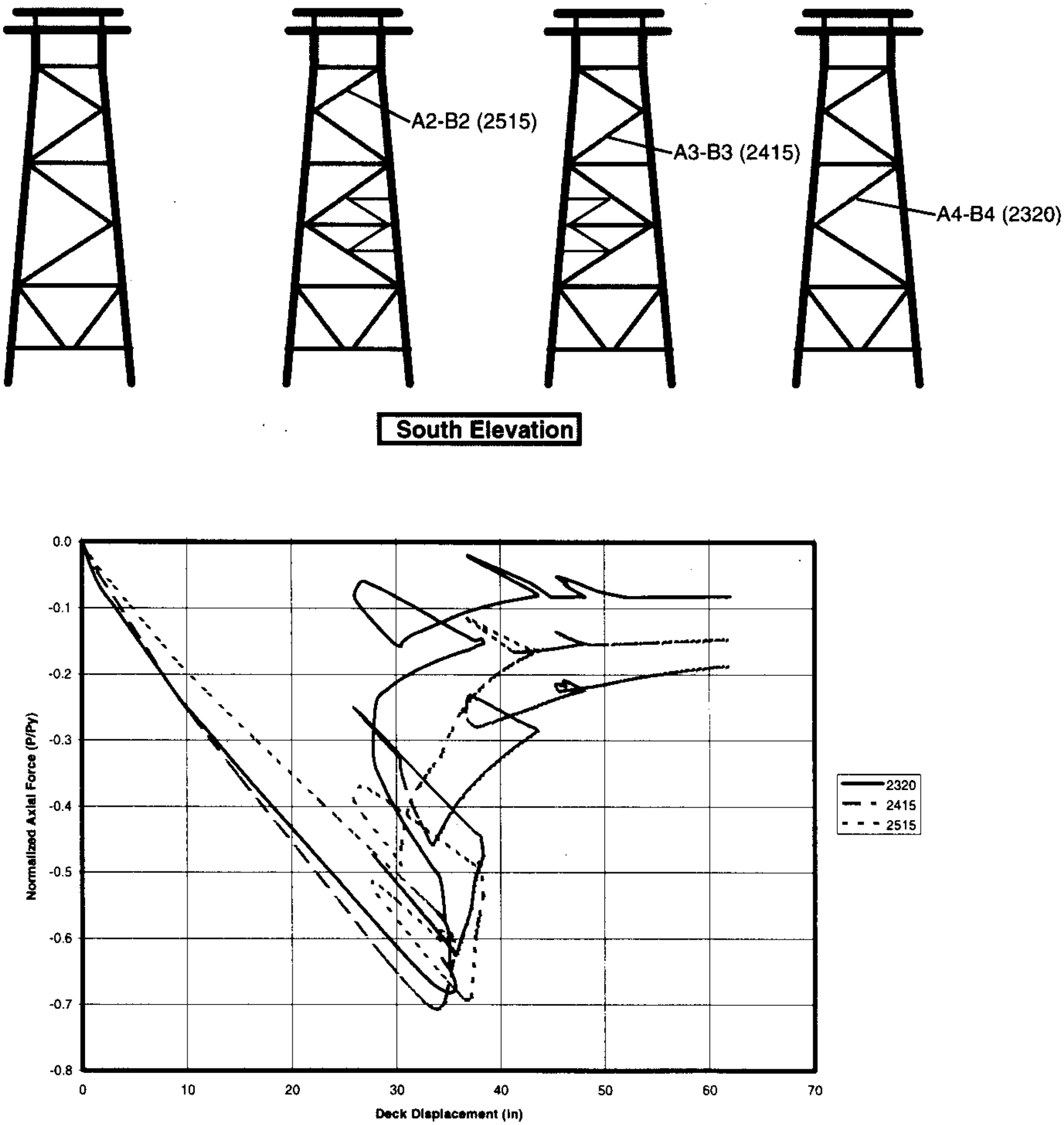

Figure 2.3.5.2-3: Critical Braces
Axial Force vs. Cellar Deck Displacement
67 ft Broadside Wave (West Traveling)

should be noted that the solution indicated yielding in other members prior to the initiation of collapse.

2.3.6 Comparison with Observed Performance

As noted previously, Ship Shoal 274A was subjected to extreme environmental loads well in excess of original design loads when Hurricane Hilda passed through the region in 1969. The maximum lateral loadings developed during Hilda were estimated to be 3500 kips to 4000 kips. Van de Graaf and Tromans (1991) estimated the maximum total lateral loadings developed during Hilda to be 3600 kips.

The results of the ULS evaluation indicate that SS274A would likely have survived Hilda with some damage (end-on lateral static loading capacity of 4570 kips). Consideration of the dynamic loading - nonlinear response characteristics of SS274A (Bea, Young, 1993) indicate an expected dynamic nonlinear loading capacity factor of $F_v = 1.1$ for this platform. These results indicate that the platform could be expected to have an ultimate dynamic lateral loading capacity of about 5000 kips.

The analyses performed by van de Graaf and Tromans (1991) indicated that this platform had a total lateral loading capacity of approximately 4800 kips when the foundation failure modes were suppressed. These results are in excellent agreement with those developed here. In addition, as was found during these analyses, van de Graaf and Tromans (1991) found that conventional static pile stiffness and capacity characterizations gave unreasonable results. Their results indicated that the platform would fail in the foundation (laterally and axially) at the maximum loadings estimated to have occurred during Hilda. These failures were indicated to occur prior to any failures in the jacket. This result was not in agreement with the results of the platform inspections that were performed following Hilda. Lateral and axial pile failure had to be suppressed before reasonable results could be obtained.

The exact nature of the damage recorded following Hilda is not readily evident based on the results of the ULS analyses performed during this study. Consequently, a more detailed examination of the results was developed. A summary of this development follows.

If the damage to brace A2-B2 occurred during Hilda, this would be confirmed by the analysis results. However, it is unclear as to whether this is the result of a separate event; van de Graaf and Tromans, 1991, assumed the damage was due to the loadings developed during Hilda.

The failures noted in first bay braces A3-B3, B2-B3 and B1-B2 are most likely due to low cycle fatigue failure and fracture. In each case, the members suffered

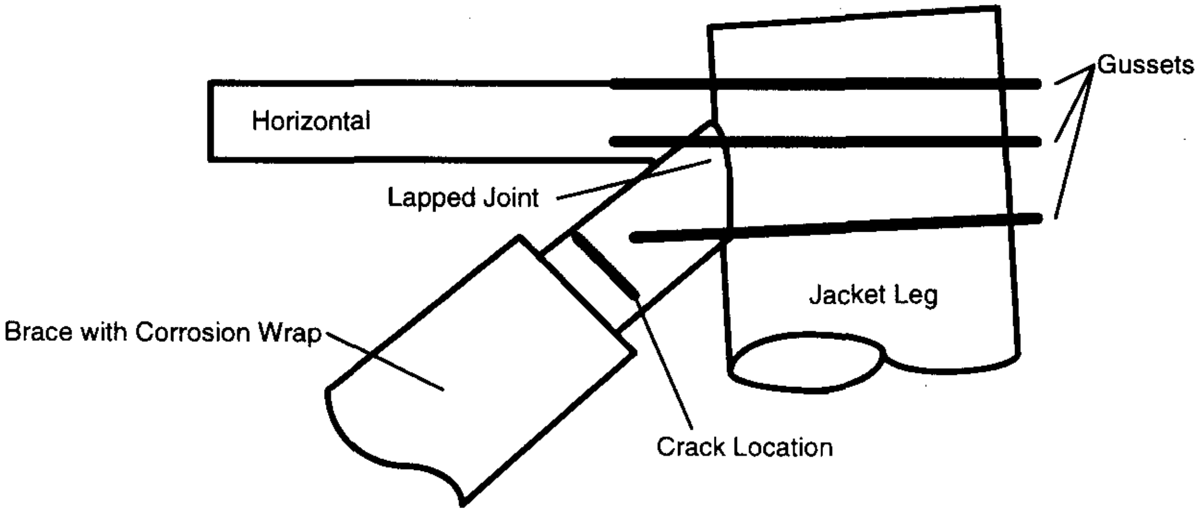

Figure 2.3.6-1: Typical Configuration of Cracked Joints

cracking just above the corrosion wrap near the brace ends (see Figure 2.3.6-1); this configuration of wrapped members and lapped brace joints stiffened by gussets is notorious for resulting in extremely high stress concentrations conducive to crack formation. Current API guidelines recommend a stress concentration factor of no less than 6 for lapped configurations (API, 1993). Stress values at the brace ends which cracked for the three first bay diagonal braces are listed below, along with the load cases corresponding to the state of stress:

A3-B3	25 ksi	Broadside, LF=0.85
B2-B3	-15 ksi	End-On, LF=0.85
B1-B2	-13 ksi	End-On, LF=0.85

The reduced load factor was used to estimate the maximum stresses associated with hurricane Hilda and to reflect the fact that the load at which these failures occurred was not due to the extreme (67 ft) wave used in the study. Given a likely stress concentration factor in the range from 5-10, and assuming 10 significant stress cycles, it would appear A3-B3 would stand an excellent chance of initiating a crack during an extreme loading event such as Hilda. B2-B3 and B1-B2 seem less likely to suffer cracking, but the chances of such an event are still reasonable.

For the damage to the upper portions of legs A1 and A3, it is apparent there was local buckling of the leg shell. Stresses in each leg segment at -10 ft MGL are shown below, along with the load case used:

A1	-28 ksi	Broadside, LF=0.85
A3	-28 ksi	Broadside, LF=0.85

Local buckling is a complicated phenomenon which is quite sensitive to material imperfection and member eccentricities (Galambos, 1988), consequently it is rather difficult to predict. API guidelines (Section 2.3.2) indicate stresses should not exceed 33 ksi for 36 ksi steel sections with D/t=92; using the assumed yield of 43 ksi would mean an upper limit of 40 ksi for local buckling prevention with this same D/t ratio. Given the moderate diameter-to-thickness ratio of the legs at this location, coupled with the presence of the corrosion wrap above and a joint can below each section, it seems possible that local buckling would indeed take place.

Overall, the results of the ULS evaluation are a good reflection of the lateral load capacity and performance of SS274A. The types of local failures which occurred normally will not be exposed during a static pushover evaluation of the type performed during this study. Even if care is taken to perform detailed checking of local failure phenomenon, there are many uncertainties which make the prediction and assessment of local failures very difficult. This should be taken as a warning that a ULS evaluation of the type performed will not always catch all possible modes of damage and/or failure which may occur; hence, good engineering judgment will be needed in order to identify problem areas a computer simulation may ignore.

3.0 PARAMETRIC STUDIES

In addition to performing the ULS verification studies, several areas of the ULS analysis process were studied parametrically. Two of these areas, that of modeling of foundation piles and the effects of member imperfection on the ULS, have already been addressed by Loch and Bea (1995). The third area, that of determining the effects of horizontal framing on the ULS, is of importance with regards to a key assumption in the program ULSLEA (Mortazavi, Bea, 1994), which is that the presence or lack of horizontal framing above and below each jacket bay in a template-type structure does not affect first member failure in that bay.

3.1 Modeling Foundation Piles

Difficulties in modeling the behavior of foundation piles have been well-documented in numerous sources as summarized by Loch and Bea, 1995. During the performance of the ULS analyses of SP62A and SS274A, preliminary results based on static pile lateral and axial characteristics indicated that the pile foundations were failing in both platforms. In light of historical data on both structures, it was judged this was unrealistic. Hence, modifications were made to the foundation elements to recognize site soil sampling, testing, analysis, and dynamic - cyclic loading effects (Loch, Bea, 1995).

For SP62A, the initial analyses indicated that the foundation piles were failing through plunging and pullout. This was most evident for the case of broadside wave attack. In recognition of soil sampling, testing, analysis and dynamic - cyclic loading effects, the foundation elements had their axial strengths factored up by 50%. Force-displacement relations for the foundation springs are summarized in Figure 3.1-1. A plot of global load vs. displacement for the analysis using the modified foundation has been overlaid on a similar plot for an analysis which uses unmodified foundation elements (Figure 3.1-2). It should be noticed from the two plots, however, that while the displacement history of the platform has changed substantially, the peak load capacity of the platform has not changed to any great extreme.

For SS274A, the structure was found to undergoing unrealistically large lateral displacements at the mudline. This was due in part to the fact the foundation was failing laterally, but also because the stiffness of the foundation elements was very low. Hence, in recognition of the soil sampling, testing, analysis, and dynamic - cyclic loading effects the foundation elements lateral capacities were factored up by 50%. In addition, the stiffness of the elements were increased by a factor of 4. Force-displacement relations for the foundation springs are summarized in Figure 3.1-3. Plots of global load vs. cellar deck displacement for SS274A using both sets of foundation elements are summarized in Figure 3.1-4. Again, it should be noted that while the displacement behavior is much more reasonable, the overall load capacity of the platform has not changed significantly.

These two incidents served to highlight the difficulties associated with accurately modeling foundation behavior. Soil sampling and testing procedures, analytical procedures, and dynamic - cyclic loading effects on pile behavior all contribute to the difficulties associated with modeling a foundation realistically.

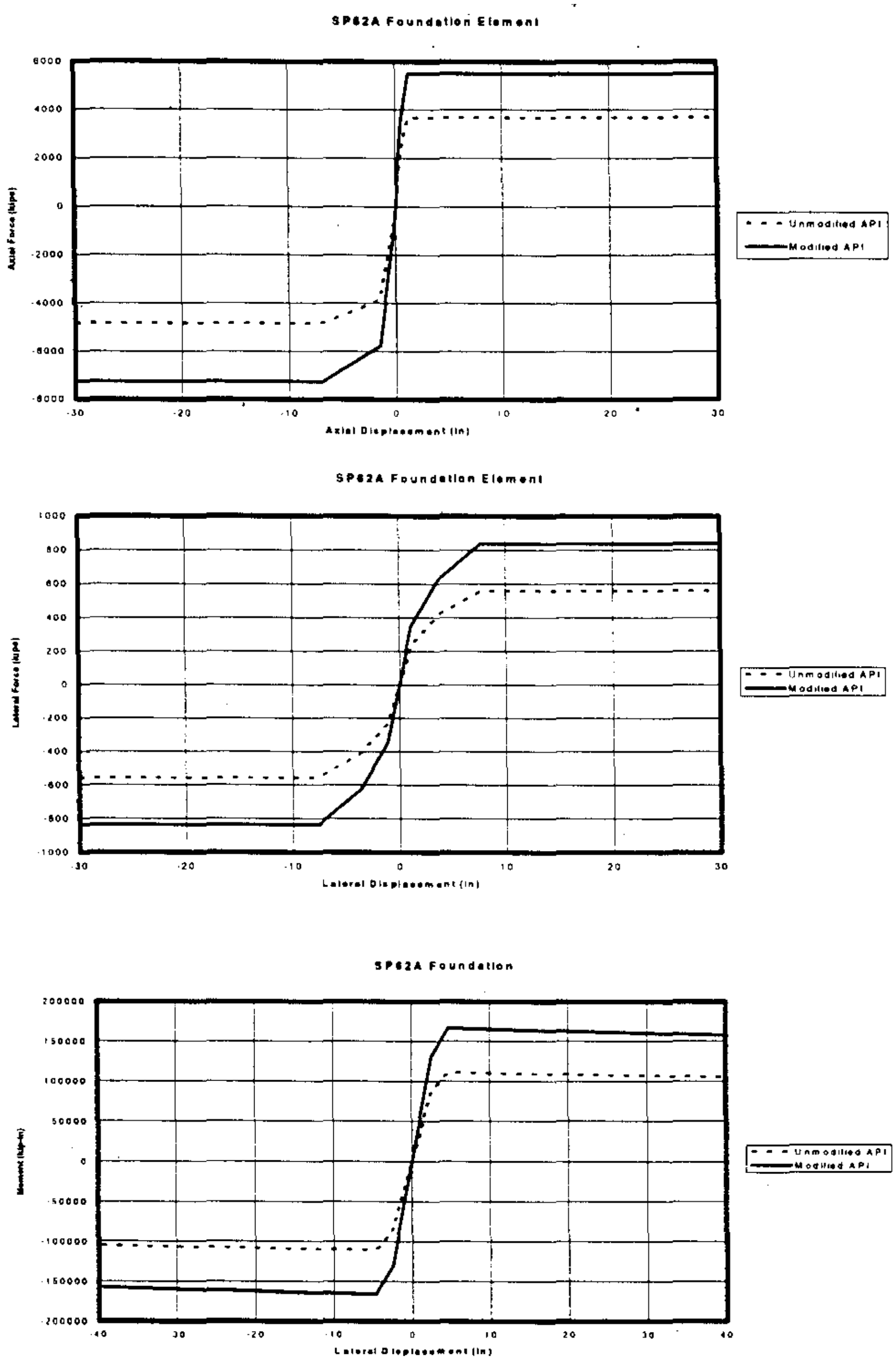

Figure 3.1-1: SP62A Spring-to-Ground Foundation Element Force-Displacement Relations

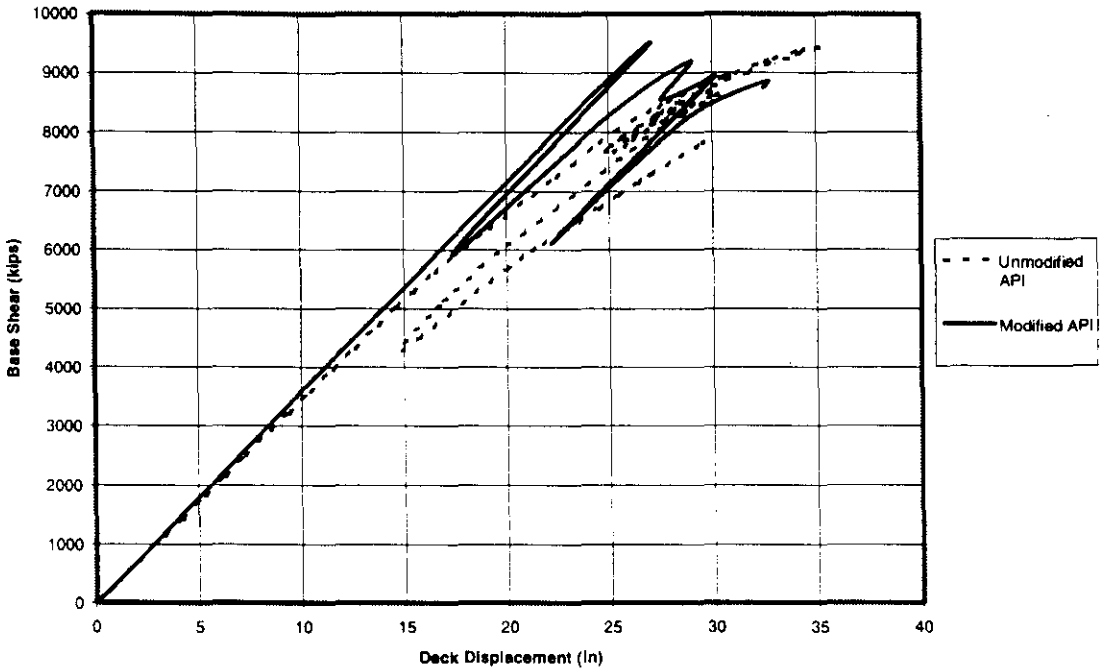

Figure 3.1-2: Comparing Effects of Modified and Unmodified API Foundations on Global Behavior of SP62A

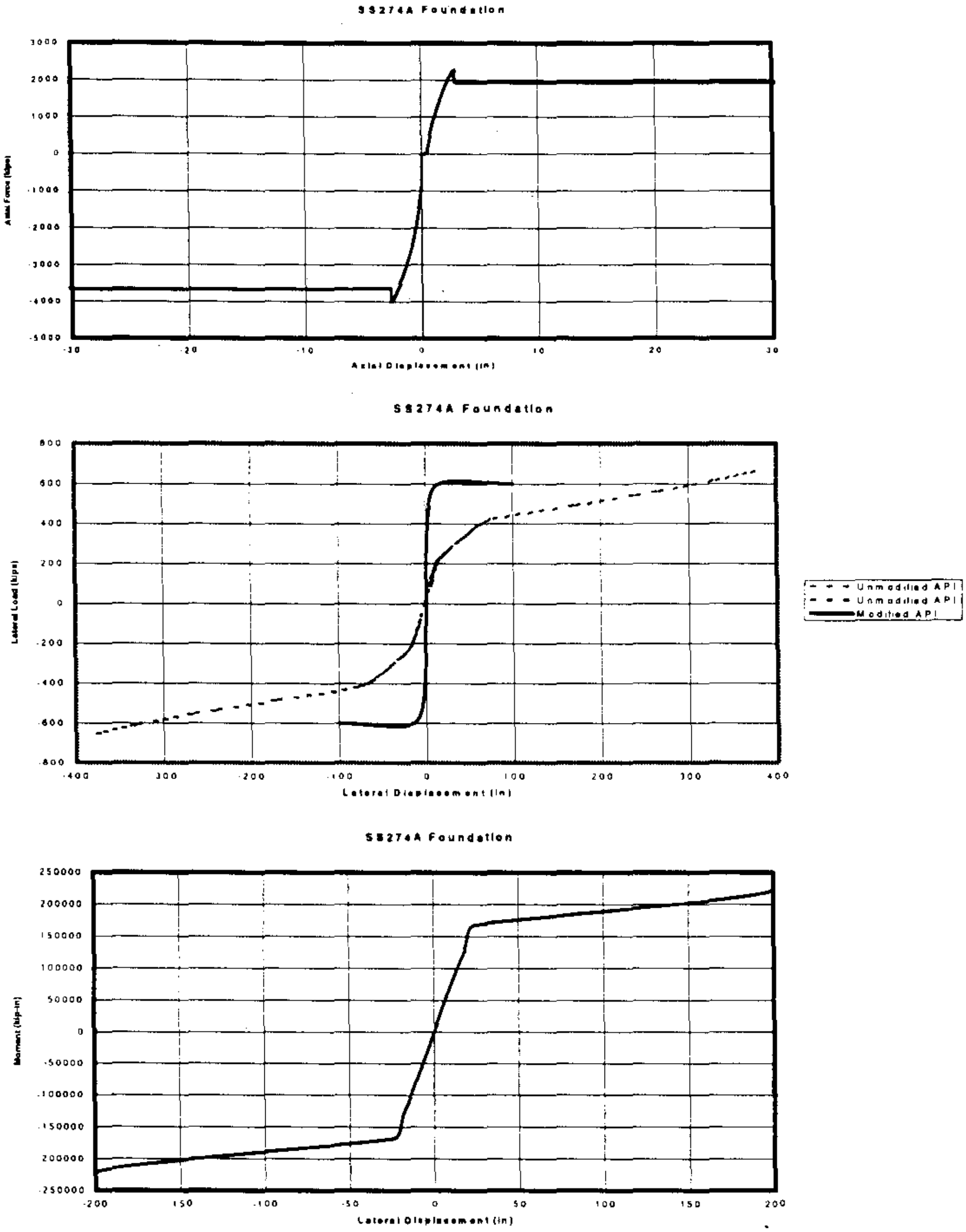

Figure 3.1-3: SS274A Spring-to-Ground Foundation Element Force-Displacement Relations

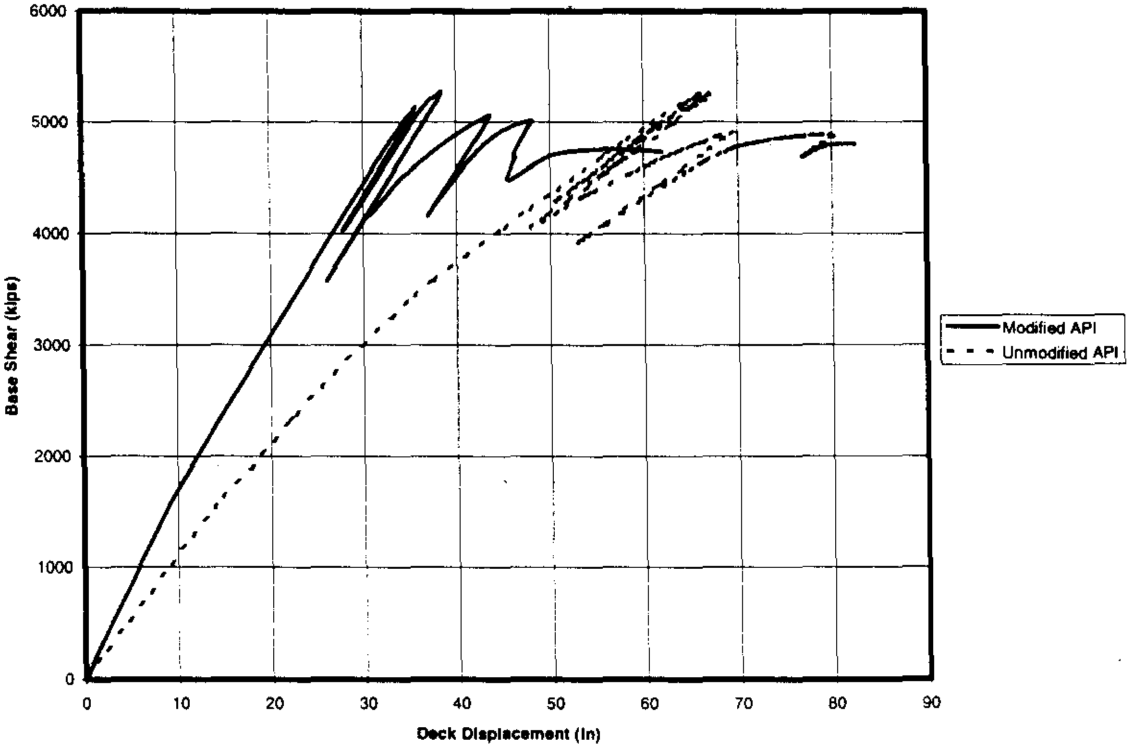

Figure 3.1-4: Comparing Effects of Modified and Unmodified API Foundations on Global Behavior of SS274A

3.2 Diagonal Brace Imperfections

Diagonal bracing in jacket structures is designed to primarily resist axial load. Hence, the strength of a diagonal brace can be characterized by both its strength in tension and its stability in compression.

USFOS allows a user to input an initial imperfection to members in order to account for their out-of-straightness. The effects of imperfection size and orientation were explored in some detail by Loch and Bea (1995). As part of a continuation of this effort, it was decided to study the effects of varying critical member orientation and size for an analysis of SP62A.

As mentioned previously, initial member imperfection was set at 0.0015L, with the imperfection in the direction of the applied load. Over a series of analyses utilizing the end-on wave attack load pattern, member imperfection was varied from 0.003L (with the load direction) to -0.003L (against the load direction). The results of this variation on the load factor at collapse may be seen in Figure 3.2-1.

Keeping in mind the original load factor for SP62A at collapse was 1.05, it can be seen that varying the member imperfection and orientation can change the resulting collapse load by at much as 15%. This is a very significant amount; it should be clear that simply increasing imperfection size without paying heed to the orientation of the imperfection may produce analytical results which are unconservative.

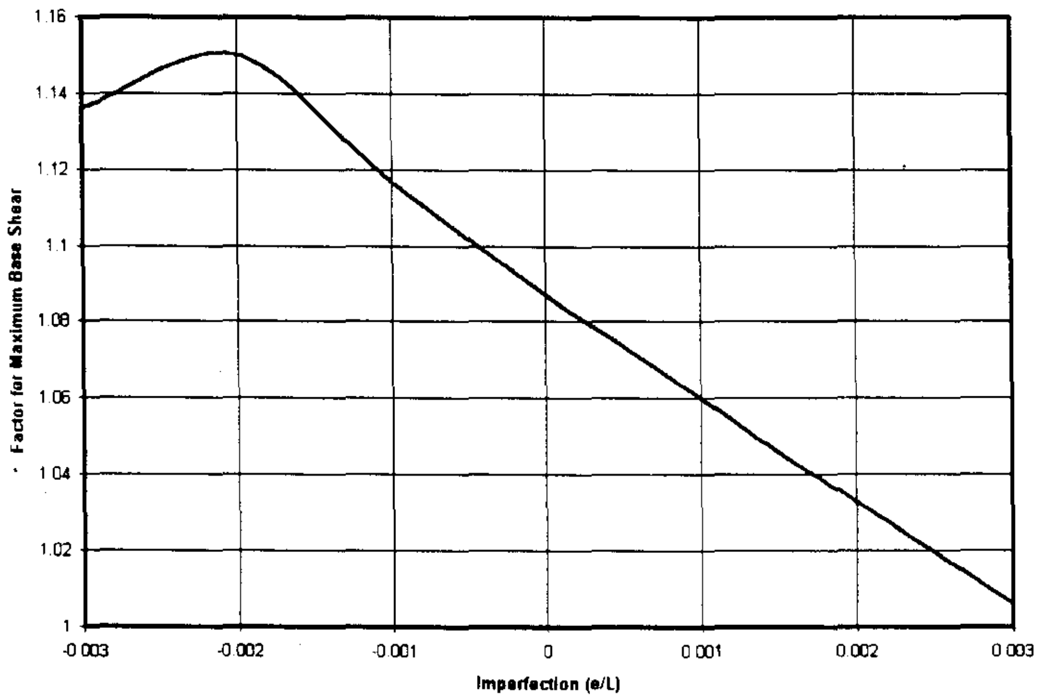

Figure 3.2-1: Effect of Brace Imperfection on Load Factor at Collapse

3.3 Effect of Horizontal Framing on ULS

Of particular interest to the development of ULSLEA (Mortazavi, Bea, 1995) is determining the effects of horizontal bracing on the ULS of steel template-type platforms. A fundamental assumption the ULSLEA program uses when evaluating the strength of diagonal braces in jacket bays is that each bay is supported by rigid framing top and bottom, regardless of whether there is actually sturdy horizontal framing at each level; it is believed the presence or lack of this framing will not influence first member failure. Hence, each jacket bay is essentially evaluated as a braced portal frame, as shown in Figure 3.3-1.

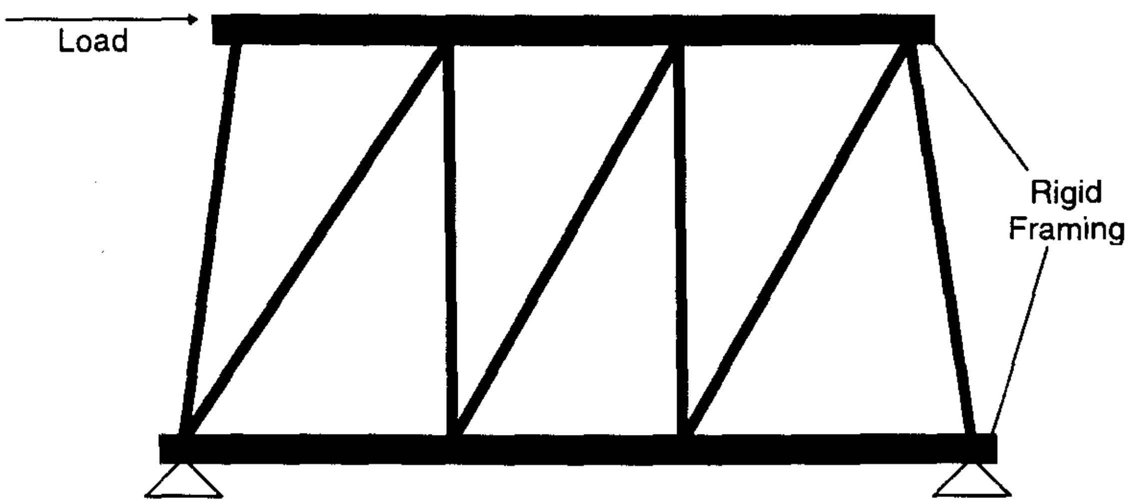

Figure 3.3-1: Portal Action for Jacket Bay

To evaluate the validity of the assumption used by ULSLEA, a study was initiated utilizing the model of SP62A. SP62A does not possess horizontal framing at every level, hence, it was decided to add horizontal members at each level between the jacket bays, and then study the effects on the ULS. The modified model may be seen in Figure 3.3-2.

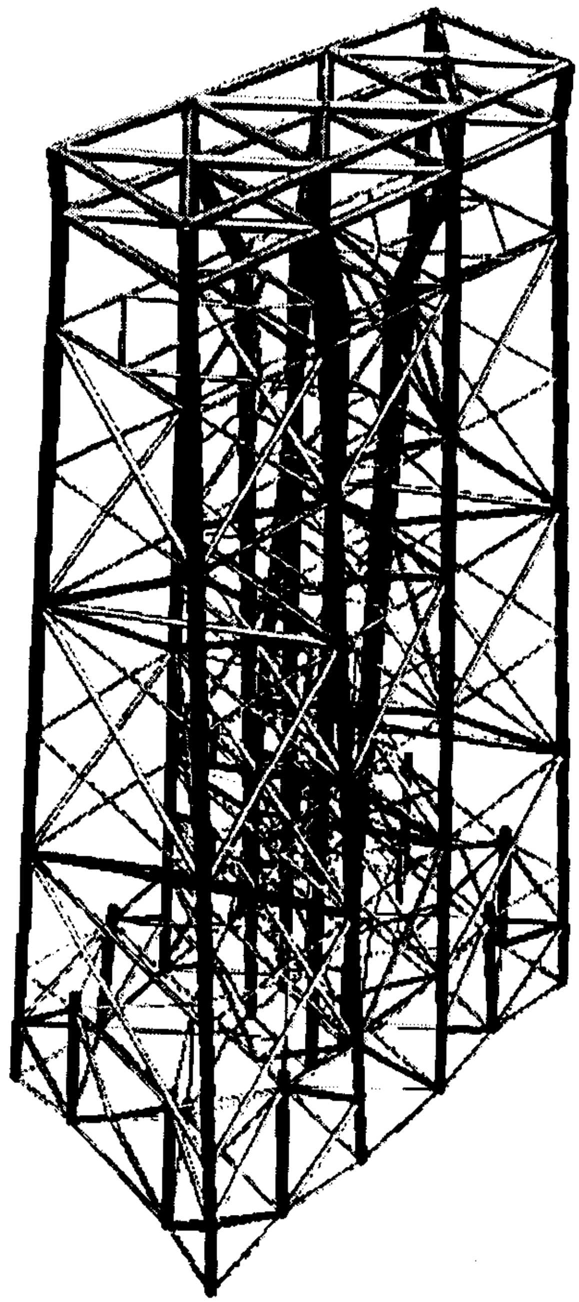

Figure 3.3-2: Isometric of Structural Model

Global results for the platform have been plotted in Figures 3.3-3,4,5 for wave attack from all three principal directions. For the case of end-on wave attack, the structure's ultimate load capacity has not changed, but the amount of residual strength has increased. This is due to the fact that the tension braces in the bays above and below the failed compression braces have taken up the load shed by the failed braces more effectively with the presence of the horizontal framing members. For the case of broadside wave attack (east-traveling wave), the effect of the bracing is negligible. There has been a slight increase in reserve strength, and slight increases in residual strength. The most dramatic change is seen in the case of broadside wave attack (west-traveling wave). There has been a 20% increase in ultimate capacity beyond first member failure, and the platform exhibits much higher reserve strength.

These results indicate that the assumption used in ULSLEA is a valid one. While the presence of strong horizontal members may aid in load redistribution following first member failure, it does not appear to affect first member failure, which is what ULSLEA uses to characterize platform capacity. Nevertheless, this effect should be studied further.

The results of these analyses also have significance from a design standpoint. The results from the broadside wave attack (west-traveling wave) indicate that substantial strength beyond first member failure may be obtained by providing a horizontal framing system by which load can be redistributed; similarly, the results of both this case and the end-on wave attack case demonstrate that horizontal framing can substantially increase residual

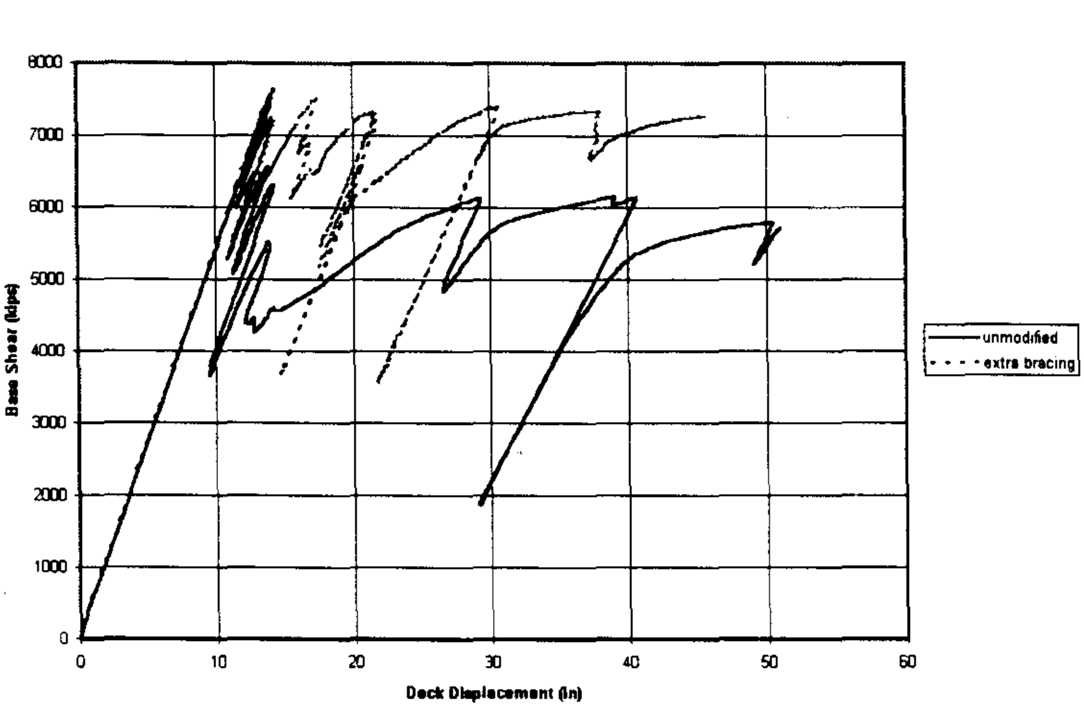

Figure 3.3-3: Effect of Additional Horizontal Framing on SP62A ULS 80 ft End-On Wave Attack (North Traveling)

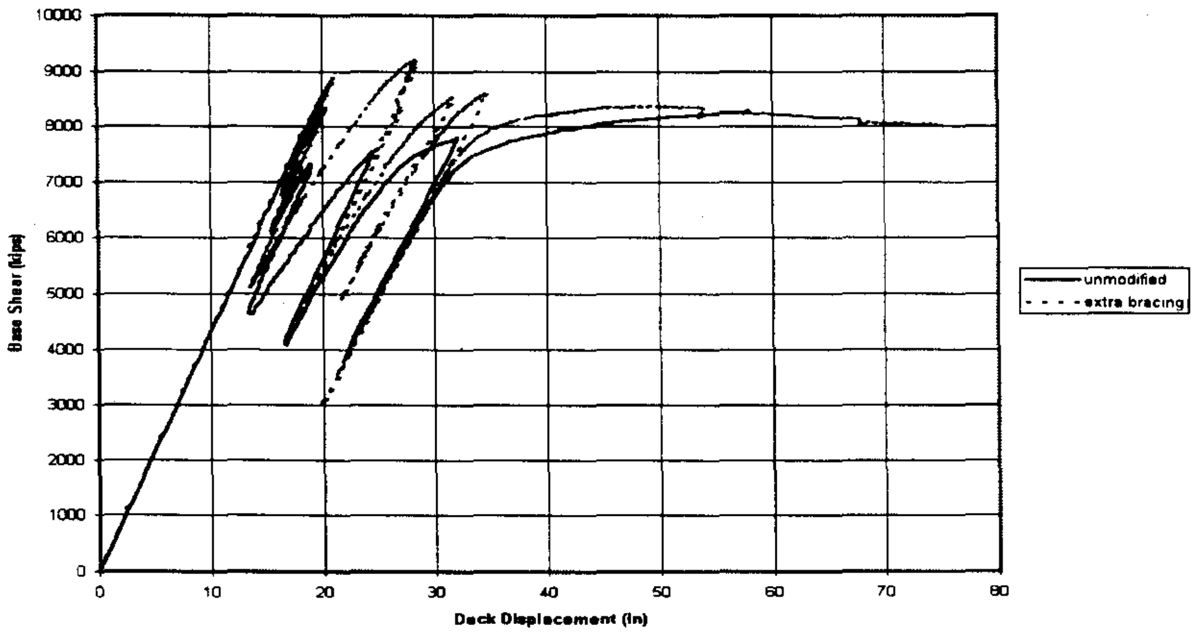

Figure 3.3-4: Effect of Additional Horizontal Framing on SP62A ULS 84 ft Broadside Wave Attack (East Traveling)

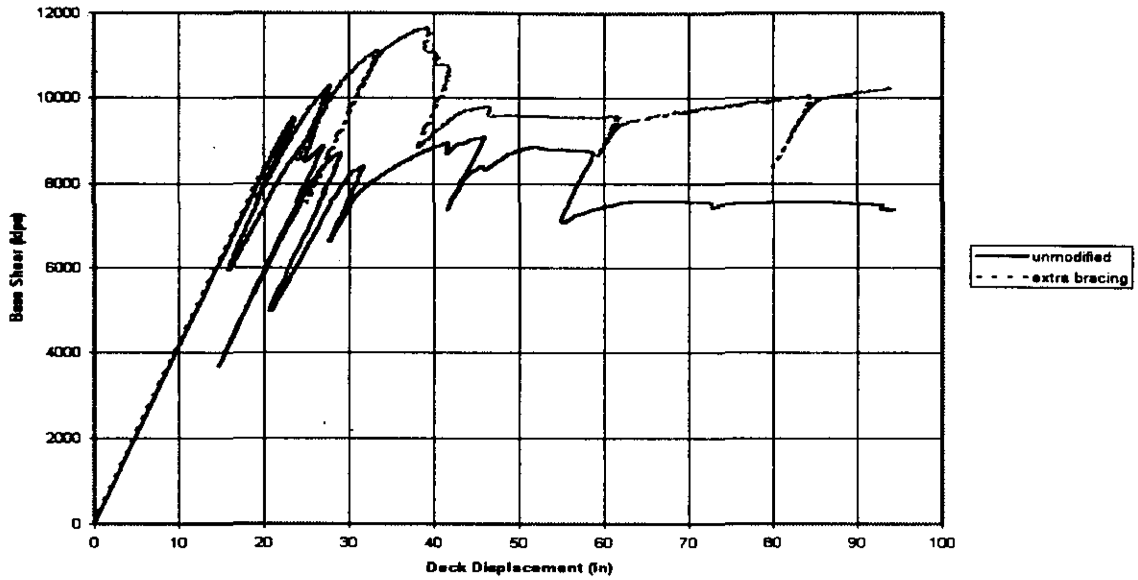

Figure 3.3-5: Effect of Additional Horizontal Framing on SP62A ULS 84 ft Broadside Wave Attack (West Traveling)

strength. Increased residual strength can have a dramatic effect on post-yield platform performance when considering the dynamic nature of the load and response (Bea, 1996); this latter issue is examined in a short study which has been appended to this report.

Both of these strength effects should not be ignored when considering methods of increasing the overall robustness and ductility of template-type structures.

4.0 CONCLUSIONS

4.1 ULS Assessments

The ULS evaluations of South Pass 62A and Ship Shoal 274A indicate both platforms possess strength substantially in excess of their original design loads. For SP62A, it was found that end-on (north-traveling) wave attack governed the ULS. The maximum static lateral load capacity was estimated to be 7440 kips. The maximum dynamic lateral load capacity was estimated to be 8930 kips. The original design load for SP62A was 3300 kips. This gives a ratio of 2.3 to 2.7 between the static and dynamic ULS capacity and the design load, respectively.

For SS274A, it was found that end-on (north-traveling) wave attack governed the ULS; the maximum static lateral load capacity was estimated to be 4570 kips. The maximum dynamic lateral load capacity was estimated to be 5030 kips. The original design load for SS274A was 1890 kips. This gives a ratio of 2.4 to 2.7 between the static and dynamic ULS capacity and the design load, respectively.

Overall, the ULS evaluations of South Pass 62A and Ship Shoal 274A indicate the validity of using detailed static pushover analyses in studying the performance of steel template-type structures subjected to hurricane wind and wave loads. The analyses indicate survival was likely for both platforms during their respective severe hurricane loadings. The results from these analyses are in agreement with the observed performance of the two structures in the hurricanes.

Evaluation of the loadings and performance characteristics of these two platforms involved extensive and very time-consuming analyses. In both cases, the initial analyses were based on conventional design basis foundation pile - soil interaction characteristics. In both cases, these characteristics resulted in unrealistic platform performance. The platforms were predicted to fail when they did not and to fail in a manner that was not consistent with post hurricane inspections.

The failures that were found in SS274A following Hurricane Hilda did not manifest themselves at the level of detail initially considered in the analyses. It took a more detailed evaluation of the forces acting on the jacket members and the stresses induced in the members in order to determine the failure modes. While detailed ULS analysis is certainly a useful tool for the evaluation of structural performance, it must be applied carefully by experienced engineers in order to ensure the results are worthwhile.

4.2 Difficulties and Conservatisms Identified

The most notable difficulty in performing the ULS evaluations described herein was the entry of extensive data into the computer. This was by no means an easy process; errors were made, but could often not be discovered until the first trial analyses were completed. Also, in several cases it took judgment on the part of the analyst to determine what was a valid result and what was not; a means of checking the results of the detailed analyses would be helpful and at least inspire confidence in the results. The program ULSLEA offers the possibility of being used to make a coarse assessment of structural performance, against which more detailed analyses may then be compared. In this fashion, erroneous results in the detailed analysis due to data errors may quickly be screened out.

Non-linear analysis programs such as USFOS have many features available to the user; these features must be used with great care to ensure realistic results. The option of member imperfection is a perfect example; careless use could return unconservative results. USFOS also possesses joint checking options; these were experimented with, but ultimately it was decided not to use the option due to the additional solution time and disk storage space required.

In addition, USFOS has solution parameters which may be adjusted to improve the accuracy of the results. The analyst experimented with the size of the load steps taken during the analysis, as well as adjusting the maximum number of recalculations of one load step due to element unloading (when an element buckles) and changing the accepted value for overshooting the yield surface for an element which deforms plastically. These adjustments were largely made on a trial-and-error basis, relying on the judgment of the analyst to determine which settings resulted in the most believable solution. As a general rule, the load steps were somewhat large (0.01) until the point of first member failure was approached; after this point, load steps ranging from 0.005 to 0.0001 were taken. The maximum number of recalculations was set at twice the recommended value, while the yield surface overshoot was set at one-half the recommended value.

The difficulties of modeling foundation performance cannot be over-emphasized. Current conventional analytical modeling processes result in generally very conservative estimates of pile capacities and stiffnesses. However, for the purposes of requalification, a more realistic assessment of foundation behavior should be made to avoid screening out platforms because analyses indicate foundation failures. It is well-documented that many requalification analyses have identified the foundation as the common weak link in the platform system (Loch, Bea, 1995); however, it should be pointed out that there have been very few platforms lost to foundation failure during storm conditions.

4.3 Areas of Future Work and Improvement

Without a doubt, foundation modeling procedures must be improved for the purposes of requalification. The conservatisms of current code practice are well-established; procedures for evaluating or including strain rate and cyclic loading effects and other potential sources of foundation strength and stiffness increases should be reviewed and further documented. Furthermore, dynamic loading and capacity effects such as those described by Bea and Young (1993) should be developed to evaluate potential impacts on the results of static analyses. Certain load effects such as waves striking the deck behave much like an impact, and can have significant loading effects. Means of accounting for or identifying local failures such as material failures or local instability should be studied; given the complexity and uncertainty associated with these effects, a probabilistic framework would seem to be the best approach.

5.0 REFERENCES

American Petroleum Institute, "API RP 2A-WSD, Section 17, Assessment of Existing Platforms," API, April 1994.

American Petroleum Institute, Recommended Practice for Planning, Designing and Constructing Fixed Offshore Platforms - Working Stress Design, API RP 2A, 20th Edition, API, July 1993.

Bea, R.G., "Gulf of Mexico Hurricane Wave Heights," Journal of Petroleum Technology, September 1975.

Bea, R.G., "Nonlinear Performance of Offshore Platforms in Extreme Storm Waves," Journal of Waterway, Port, Coastal and Ocean Engineering, ASCE, Vol. 122, No. 2, March/April 1996.

Bea, R.G. and Young, C., "Loading and Capacity Effects on Platform Performance in Extreme Storm Waves and Earthquakes," OTC7140, Offshore Technology Conference, May 1993.

DNV, PREFRAME Users Manual, 1994a.

DNV, WAJAC Users Manual, 1994b.

Galambos, T.V. (ed.), Guide to Stability Design Criteria for Metal Structures, 4th Edition, Wiley and Sons, 1988.

Galambos, T.V. and Ravindra, M.K., "Properties of Steel for Use in LRFD," Journal of the Structural Division, ASCE, Vol. 109, No. ST9, September 1978.

Lee, G.C., correspondence to R.G. Bea regarding AIM III Project, May 1988.

Loch, K. and Bea, R.G., "Determination of the Ultimate Limit States of Fixed Steel-Frame Offshore Platforms Using Static Pushover Analyses," Report to U.S. Minerals Management Service and Joint Industry Project Sponsors, Marine Technology Development Group, Department of Civil Engineering, University of California at Berkeley, May 1995.

Marshall, P.W. and Bea, R.G., "Failure Modes of Offshore Platforms," BOSS Conference Proceedings, 1976.

Mortazavi, M. and Bea, R.G., "ULSLEA, Simplified Nonlinear Analysis for Offshore Structures," Report to Joint Industry-Government Sponsored Project, Marine Technology and Management Group, Department of Civil Engineering, University of California at Berkeley, June 1994.

Nadai, A., Theory of Flow and Fracture of Solids, Vol. 1, 2nd Edition, Engineering Society Monographs, McGraw-Hill, 1950.

Rodenbusch, G. and Kallstrom, C., "Forces on Large Cylinders in a Random Directional Flow," OTC5096, Offshore Technology Conference, 1986.

SINTEF, USFOS - A Computer Program for Progressive Collapse Analysis of Steel Offshore Structures, Users Manual v7.0, 1994.

SINTEF, USFOS - A Computer Program for Progressive Collapse Analysis of Steel Offshore Structures, Theory Manual, 1993.

SINTEF, USFOS - A Computer Program for Progressive Collapse Analysis of Steel Offshore Structures, Verification Manual, 1991.

SINTEF, POSTFOS - A Computer Program for the Interactive Presentation of USFOS Analysis Results, Users Manual v2.2, 1992.

Tromans, P.S. and van de Graaf, J.W., "A Substantiated Risk Assessment of a Jacket Structure," OTC7075, Offshore Technology Conference, 1992.

Van de Graaf, J.W. and Tromans, P.S., "Statistical Verification of Predicted Loading and Ultimate Strength against Observed Storm Damage for an Offshore Structure," OTC6573, Offshore Technology Conference, 1991.

APPENDIX

Response of an Offshore Structure to Single and Series Waves

by

James D. Stear

ABSTRACT

This paper is intended to address the differences in the response of an offshore platform to a series of waves as opposed to a single wave. A simple template-type offshore platform has been selected for evaluation (stiffness, strength, and post-yield behavior are known). The structure has been evaluated using the program MATLAB for both the case of being subjected to a series of wave and the case of being subjected to a single wave. Curves have been constructed showing ductility demand based on the height of the single wave, and the number and height of the series waves. These results have been contrasted with the actual (or assumed) ductile capacity of the structure.

TABLE OF CONTENTS

1.0 INTRODUCTION

Much attention has been directed in recent years to the analysis of offshore jacket-type structures subjected to hurricane wave loads. Current practice concentrates on the use of detailed static pushover analyses to determine a given structure's "collapse load," i.e. the maximum sustained lateral load capacity, based on a prescribed wave loading pattern. This approach assumes the structure will be rendered unserviceable after being loaded to this extreme level.

However, the static analysis approach overlooks several important aspects of the real-life performance of these structures; namely, the time-dependent nature of the loads and the structure's ability to withstand inelastic deformations (often expressed as "ductility"). Static analyses do not address the fact that the real-life load being applied to a structure is momentary, and while some overload or yielding may take place, a structure may in fact possess sufficient post-yield strength to avoid complete collapse. If some damage can be absorbed from an overload event without complete collapse, the structure may be considered marginally serviceable even though its maximum sustained lateral load capacity was exceeded. Needless to say, the next issue that would need to be addressed is the possible threat to the platform from a series of such overload events, i.e. a train of extreme waves.

This paper explores the differences in response of a typical jacket-type structure to both single and series wave attacks. An analytical model describing the behavior of the platform has been developed, and the model has been evaluated for several wave attack conditions with varied wave heights and numbers of waves. Comparisons of structural performance have been made based on two assumptions of lateral force-deck displacement ("global") behavior: elastic-perfectly plastic (EPP) and brittle/elastic-perfectly plastic (B/EPP). Ductility demands based on the response of both of these behavior models have been calculated. These results are then discussed with emphasis being placed on determining the effectiveness of the different strength behaviors at withstanding wave attacks, either single or series. Suggestions are made as to what improvements might be made in the design of these platforms so as to gain a better distribution of strength.

2.0 ANALYSIS

To evaluate the effects of dynamic loading from single and series wave attacks on jacket-type structures, a typical jacket-type structure was selected for study. This platform was modeled as a single degree-of-freedom (SDOF) system, and was studied using time-history analysis techniques to evaluate its response to wave loads. The platform characteristics are described in Section 2.1. The numerical evaluation procedure is discussed in Section 2.2, and the wave kinematics and force calculation procedures are reviewed in Section 2.3.

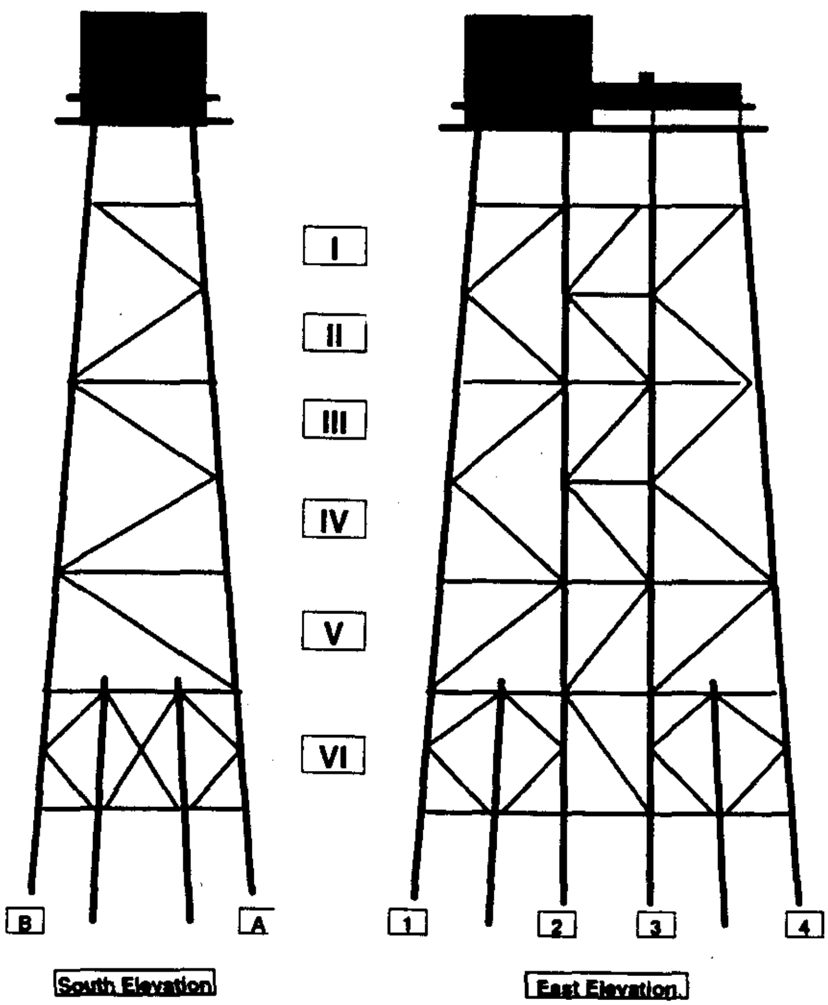

Figure 2.1.1: Shell SP62A

2.1 Sample Platform

The jacket structure selected for study is based upon an existing platform (Shell SP62A: see Figure 2.1.1 on previous); however, some modifications have been made to the characteristics of the structure. The sample platform is an 8 leg structure (legs are diameter 60 inch), and is assumed to be sited in 400 ft of water. The deck is located at +40 ft above the water's surface. Operating weights for the deck are assumed to be 10,000 kips. Damping for the structure has been taken as 3%; this value was derived from field tests performed on Shell SP62C [9].

It is assumed for the purpose of these evaluations that failure will only occur in the jacket structure; no effort will be made to account for foundation effects. Information on the strength performance of the platform is based on static pushover analyses performed on SP62A [3]. These analyses established that the limiting load case for the platform was that of an end-on wave attack, with the collapse load being achieved for an 80 ft wave (Figure 2.1.2). Following the failure of several key members (compression braces in the

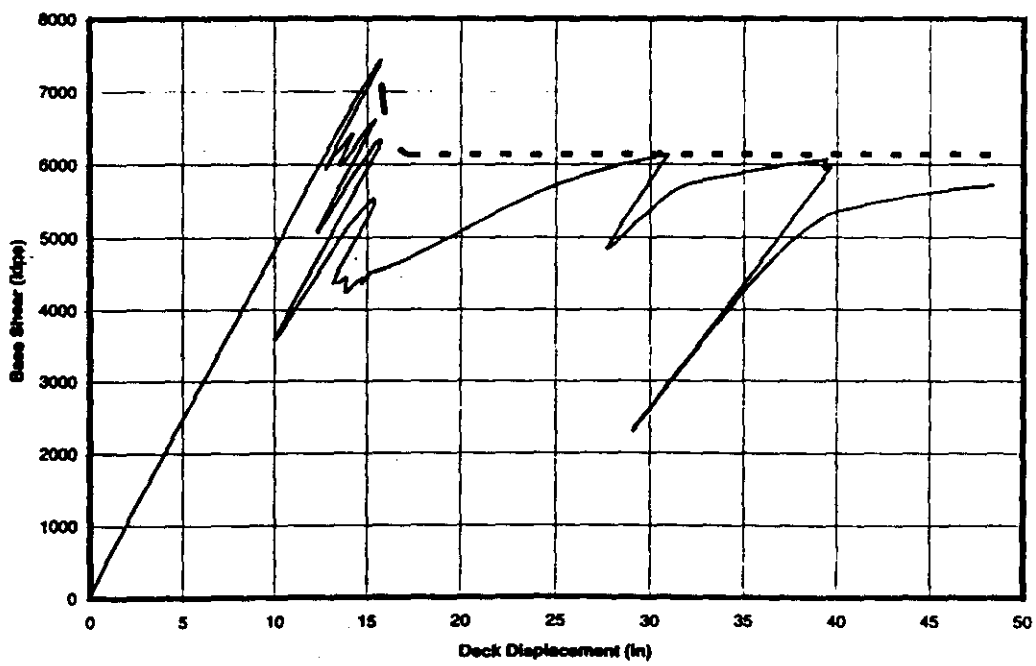

Figure 2.1.2: Base Shear vs. Cellar Deck Displacement (SP62A)

3rd and 4th jacket bays), the structure exhibits a reduced strength; load capacity at this point is limited by the amount which can be carried by the tension members and portions of the jacket legs in the bays with the failed compression members. This strength performance is characterized as "brittle/elastic-perfectly plastic" (B/EPP); the platform's collapse load is reached at first member failure. Stiffness and strength for the B/EPP case were taken from the results of this analysis.

SP62A was also analyzed in a modified condition, in which horizontal framing members were added between jacket bays 1 and 2 and bays 3 and 4 to improve load redistribution following member failures. The results of the analysis of the modified structure subjected to an end-on 80 ft wave attack indicate the global response of the platform resembles more of an elastic-perfectly plastic (EPP) behavior (Figure 2.1.3), as opposed to the B/EPP behavior previously exhibited. Following the failure of the compression braces in the 3rd and 4th jacket bays, the structure is seen to have the capability to withstand loads at the same level at which the first member failures occurred. This is due to the fact that

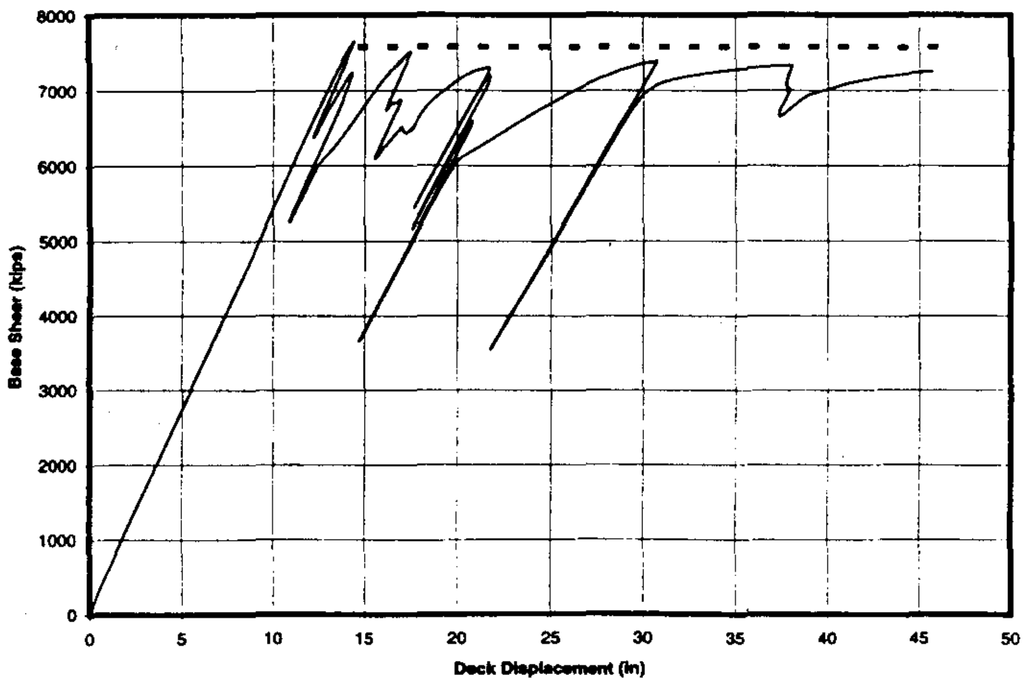

Figure 2.1.3: Base Shear vs. Cellar Deck Displacement (SP62A mod.)

the horizontal framing placed within the model allows for better transfer of the load to the tension members in the adjacent jacket bays. Stiffness and strength for the EPP case were taken from the results of this analysis.

2.2 Numerical Model for Time-History Analysis

To conduct the dynamic analysis, it was decided to model the structure as a single degree-of-freedom (SDOF) system with the deck displacement being taken as the reference coordinate. This assumes the majority of the response of the platform will be captured within the first or primary mode of the structure, and hence the deflection of the rest of the structure can be generalized with respect to the deck displacement [6,4]. The shape function for a cantilever beam was chosen to capture the deflected shape of the structure and reference it to the deck deflection:

$$\psi(x) = \frac{3}{2}\frac{x^2}{L^2} - \frac{1}{2}\frac{x^3}{L^3}$$

This shape function was used to extrapolate the distributed loads on the jacket legs up to the deck level of the model for the purposes of the analysis. The mass of the platform was considered to be lumped at the deck level.

As noted previously, the lateral force-deck displacement relationships calculated during the analysis of SP62A were used to establish global stiffness and strength values for the B/EPP and the EPP cases. Stiffness, yield strength and displacement, and post-yield strength are shown below in Table 2.2.1 for both cases.

	Stiffness (kip/in)	Yield Strength (kip)	Yield Displ. (in)	Post Yield (kip)
B/EPP	470	2500	5.3	1500
EPP	470	2500	5.3	2500

Table 2.2.1: Platform Strength Characteristics

It is obvious that the strength values and yield displacements are not identical to the collapse loads and residual strengths shown in Figures 2.1.2 and 2.1.3; this is due to the fact that it will be necessary to extrapolate the distributed loads on the jacket up to the deck level. As a cantilever beam loaded to the same tip displacement by both a uniformly-distributed load and a point load at the tip has a base shear ratio of 2.67 $shear_{uniform} : shear_{point}$, it was decided to factor the strength values of the platforms down by a factor of 3 to account for the differences in load application.

Newmark's constant average acceleration method for non-linear systems [6] was utilized to perform the integration of the equation of motion. A MATLAB routine previously written for the evaluation of a SDOF EPP system was taken and adapted for use with the case of B/EPP behavior.

2.3 Wave Kinematics and Force Calculations

Wave loads on the structure were calculated using the MJOS equation to find member forces and API guidelines to estimate deck loads. Water particle kinematics were established based on deep water linear wave theory, with horizontal velocities and accelerations being established by use of depth-stretching.

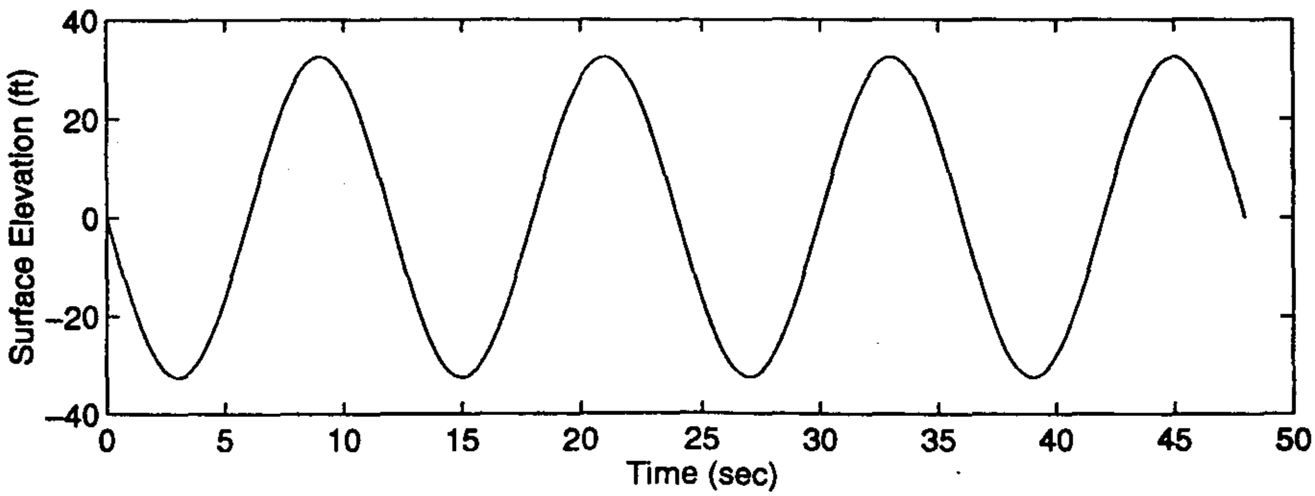

Figure 2.3.1: Surface Elevation vs. Time for a Passing 65 ft Wave

T was chosen to be 12 sec for all waves; based on deep water linear wave theory and together with the depth of 400 ft this limits the maximum (deep water) wave to a height of 115 ft. For the analysis, waves in the range from 65 ft - 115 ft were considered, with encounters with up to 4 waves in series. The wave profiles were assumed to be simple sinusoids (trough leading crest), as seen in Figure 2.3.1. For waves traveling in series, the waves were generated sequentially with no lag in between.

The following relations [2] were used to establish the water particle kinematics:

$$\eta = \frac{H}{2}\cos(\theta)$$

$$u = \frac{\pi H}{T} e^{kz} \cos(\theta)$$

$$a = \frac{2\pi^2 H}{T^2} e^{kz} \sin(\theta)$$

The acceleration and velocity were reduced using a wave kinematics factor of 0.866 [2].

Wave forces on the jacket members were calculated based on the MJOS equation, as shown below [2]:

$$F = C_d \frac{\rho}{2} D u|u| + C_m \rho \frac{\pi D^2}{4} a$$

The drag coefficient, C_d, and inertia coefficient, C_m, were chosen as 1.2 and 1.5 respectively, based on [8]. These forces were then integrated together with the shape function referenced to the generalized coordinate in order to estimate the forces appropriate to a single jacket leg:

$$\tilde{p}(t) = \int p(z,t)\psi(z)dz$$

To account for the absence of force calculations on members other than the jacket legs, it was decided to double the load calculated on the 8 jacket legs. Also, it was assumed the velocity and the acceleration of the structure as it moved under the wave loads would be very small compared to the velocity and acceleration of the water particles; hence, no relative motion calculations would need to be performed. This assumption simplifies the calculation immensely, and is reasonable to make [5].

Loads on the deck of the structure were calculated according to API guidelines governing the requalification of offshore structures for continued service [1]:

$$F = \frac{\rho}{2} C_{ddeck} Area|u|u$$

C_{ddeck} was chosen to be 2.5, representative of a heavily-cluttered deck. These forces were applied directly to the model with no modification, as they occur at the level of the deck.

To gain a sense of the magnitude of the deck load contribution, plots of applied force vs. time are shown in Figures 2.3.2 and 2.3.3 for two cases: four 65 ft waves and four 95 ft waves. Obviously, the wave forces on the deck make a substantial contribution to the overall load on the structure.

Several aspects of the wave force calculations should be commented upon before proceeding. It should be noted that it would be better to "ramp up" the wave height over time when performing the time-history analysis, as this will prevent a sudden pulse being applied to the structure from the high inertial forces existing at the front of the wave trough. It may also be worthwhile to experiment with different wave theories, in order to determine the effects on load calculation based on different kinematics.

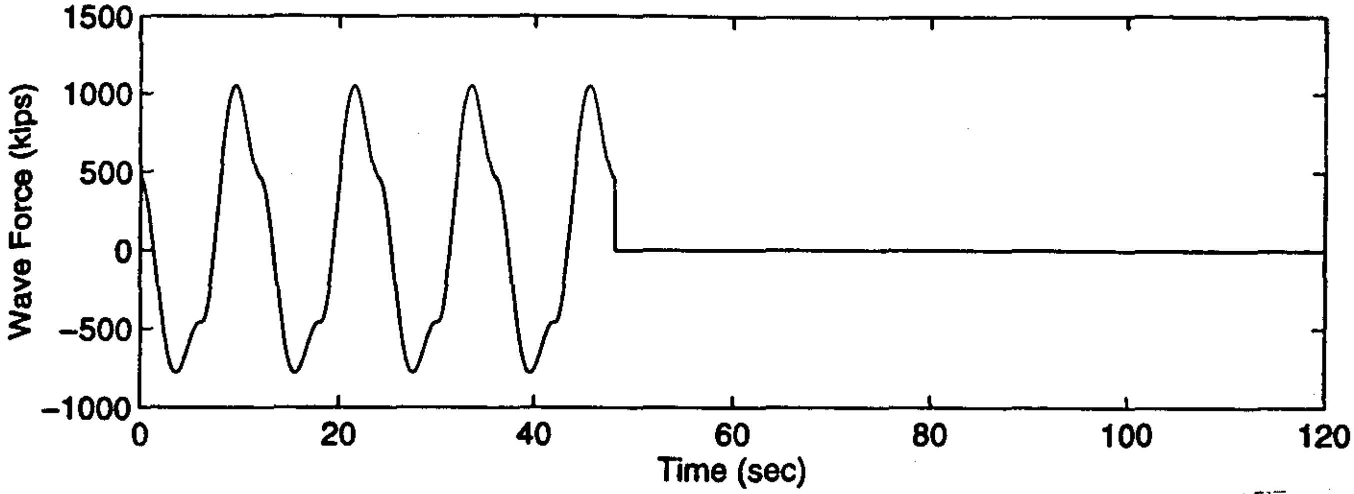

Figure 2.3.2: Wave Force vs. Time, 65 ft Waves

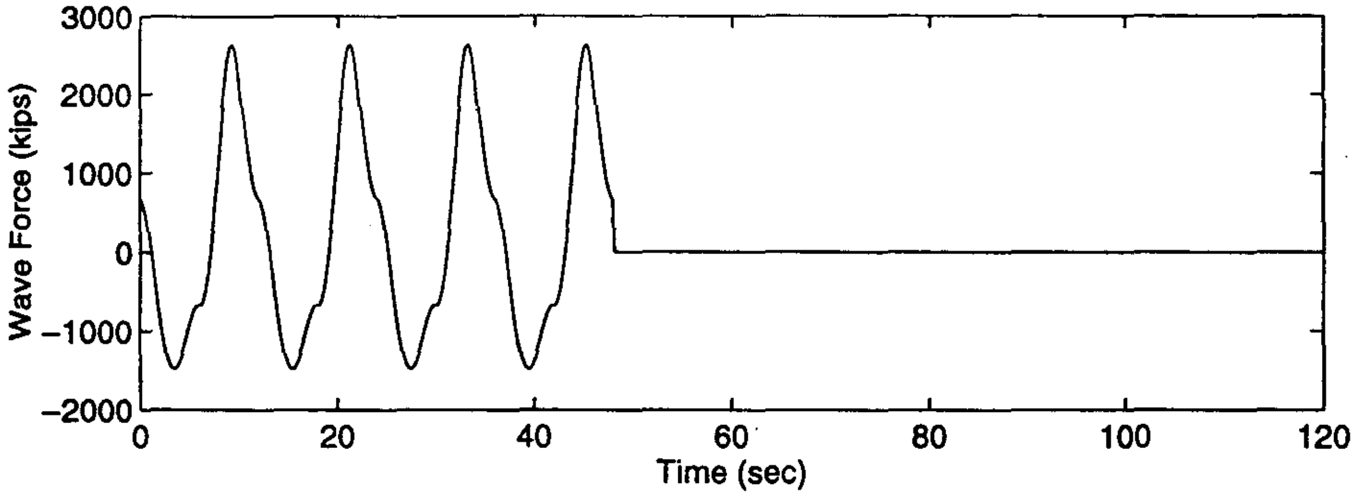

Figure 2.3.3: Wave Force vs. Time, 95 ft Waves

3.0 ANALYSIS RESULTS

Each model was analyzed for the following load cases: Wave heights of 65, 75, 85, 95, 105 and 115 ft, and numbers of waves ranging from one to four.

To gain general insight as to the relative performance of the B/EPP structure and the EPP structure, plots were made of ductility demand (defined as the maximum structure deck displacement divided by the displacement of the deck at yield) for both models (see Figures 3.1 and 3.2). For the cases of wave attack by 85 ft waves and smaller, neither structure appears to be in danger, as both exhibit elastic behavior. However, it is for the cases of wave attack by waves of 95 ft and larger that the differences in robustness between the two structures become apparent. Beyond waves with heights of 85 ft, the B/EPP structure is in danger of being destroyed by a single wave encounter. The EPP structure, however, does not appear to be in danger until encounters with waves of 105 ft and larger.

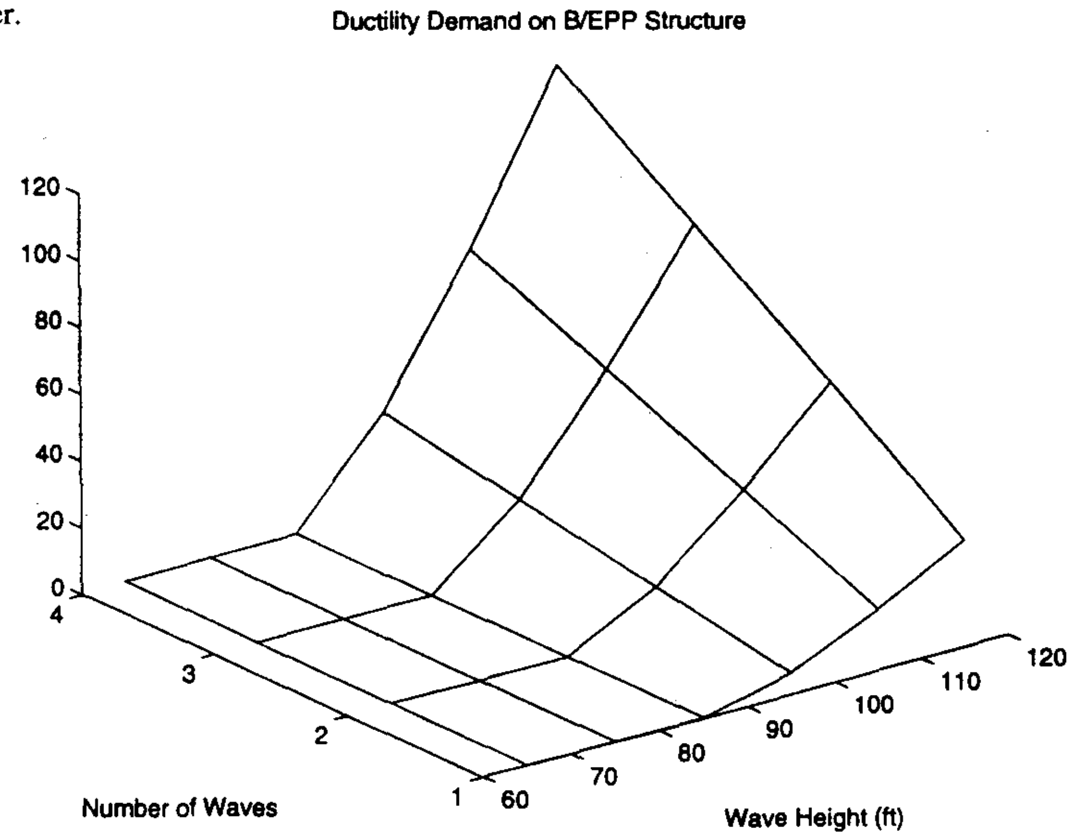

Figure 3.1:

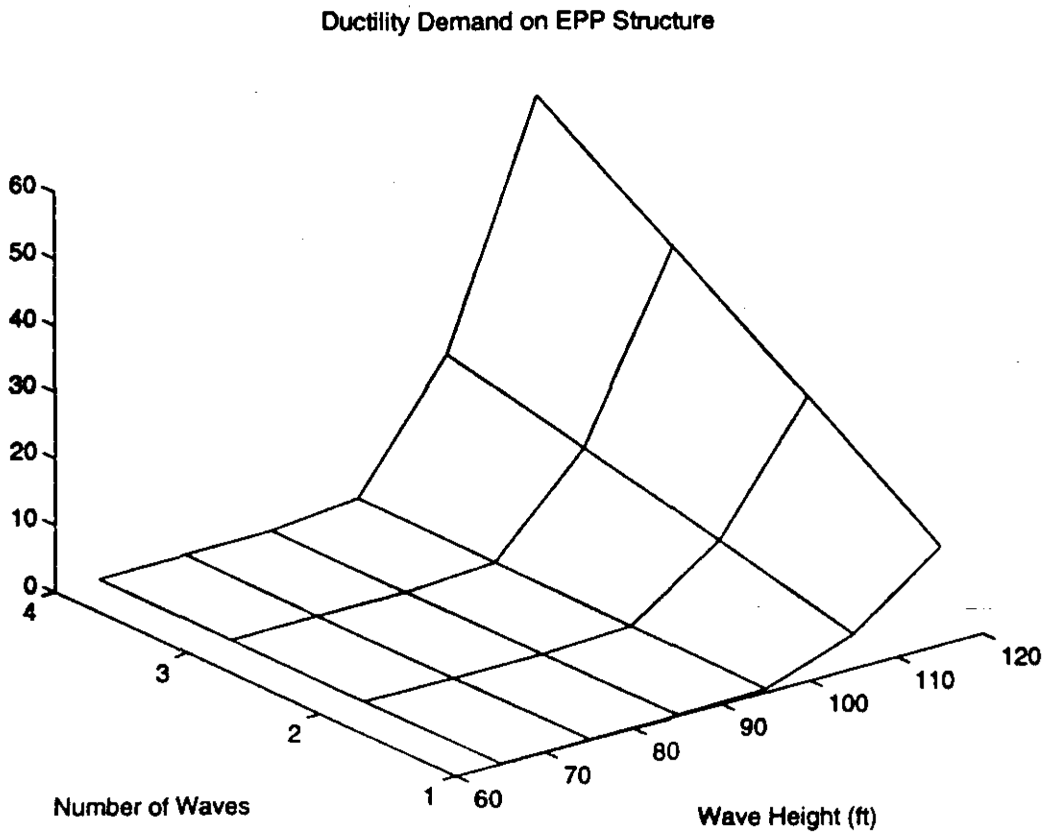

Figure 3.2:

To obtain a more detailed comparison between the two structures, plots of deck displacement vs. time were made for each system for the cases of both a single 95 ft wave attack and a series of three 95 ft waves. These plots are shown in Figures 3.3-3.6. In addition, plots of structural resisting force vs. deck displacement have been made for each structure for the case of an attack by three 95 ft waves (Figures 3.7-3.8). Clearly, for both load cases it is unlikely the B/EPP structure would have survived. The ductility demand on the structure is between 20 to 60; at most it would be reasonable to expect a structure of this type to have a ductile capacity of 10. The EPP structure, however, is at most subjected to a ductile demand of 5, which it could most likely survive, although in a damaged state. The importance of avoiding a sudden drop in structural strength due to damage should be clear.

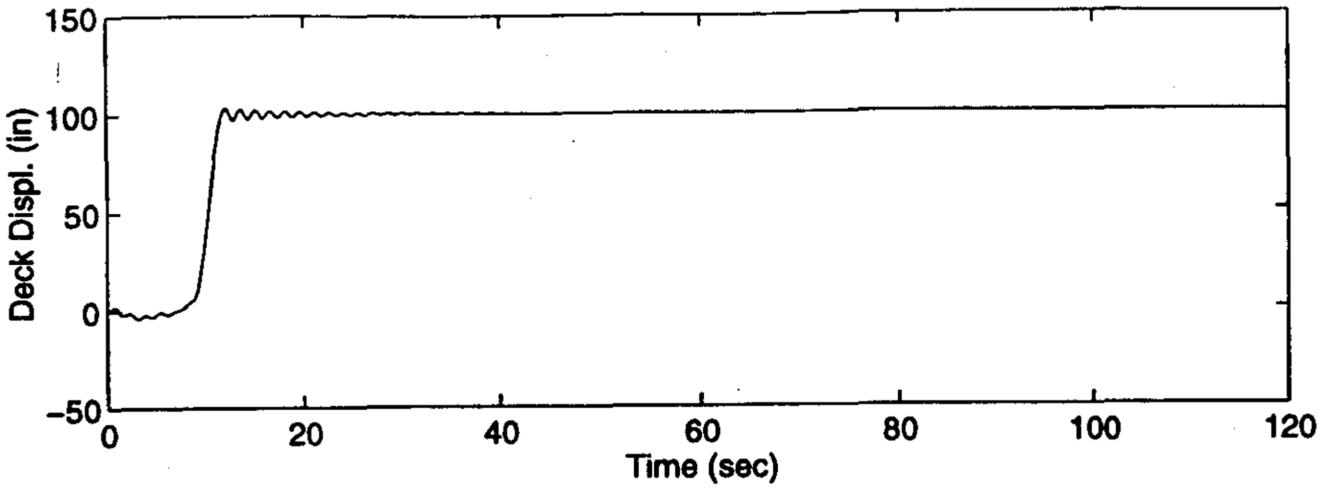

Figure 3.3: B/EPP Deck Displacement vs. Time, Single 95' Wave Attack

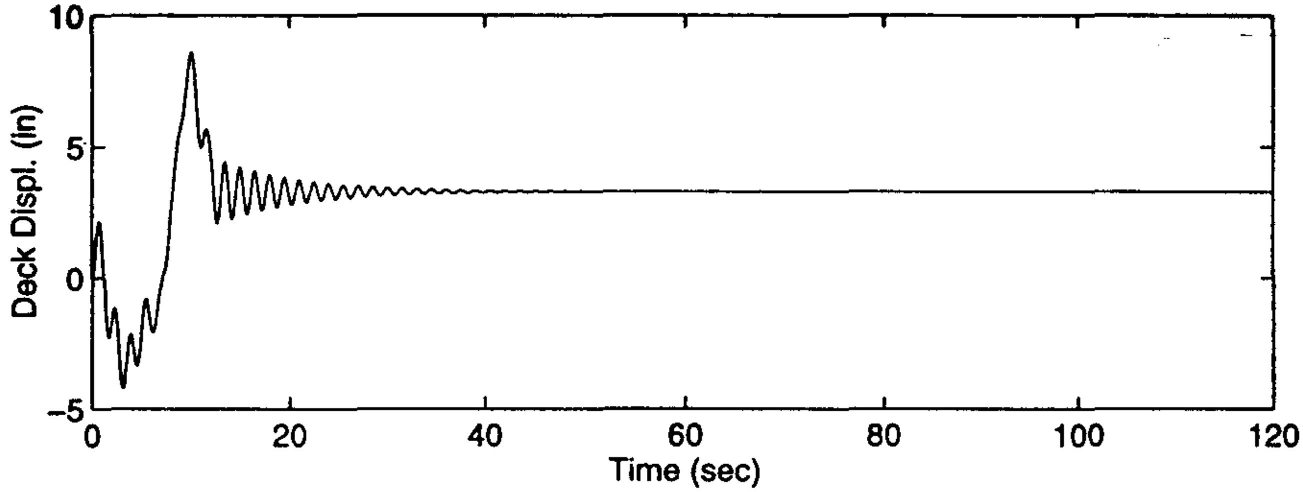

Figure 3.4: EPP Deck Displacement vs. Time, Single 95' Wave Attack

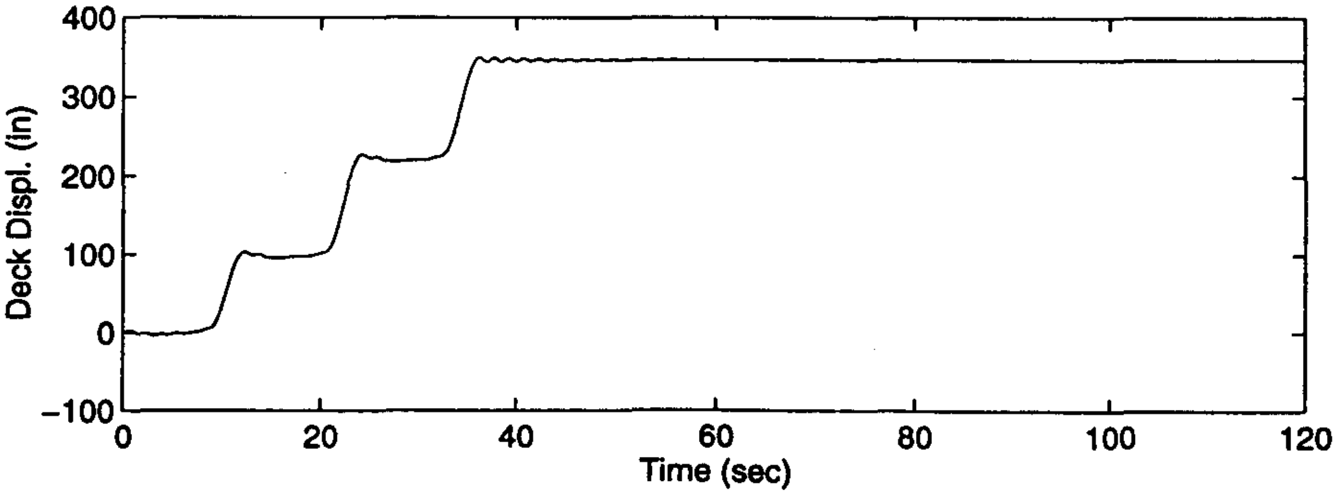

Figure 3.5: B/EPP Deck Displacement vs. Time, Series 95' Wave Attack

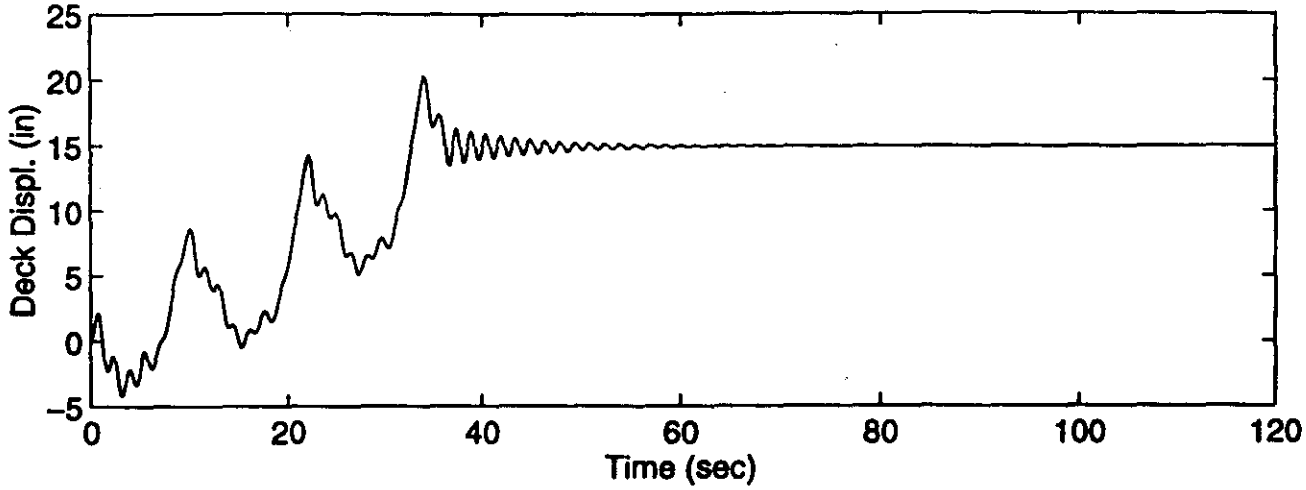

Figure 3.6: EPP Deck Displacement vs. Time, Series 95' Wave Attack

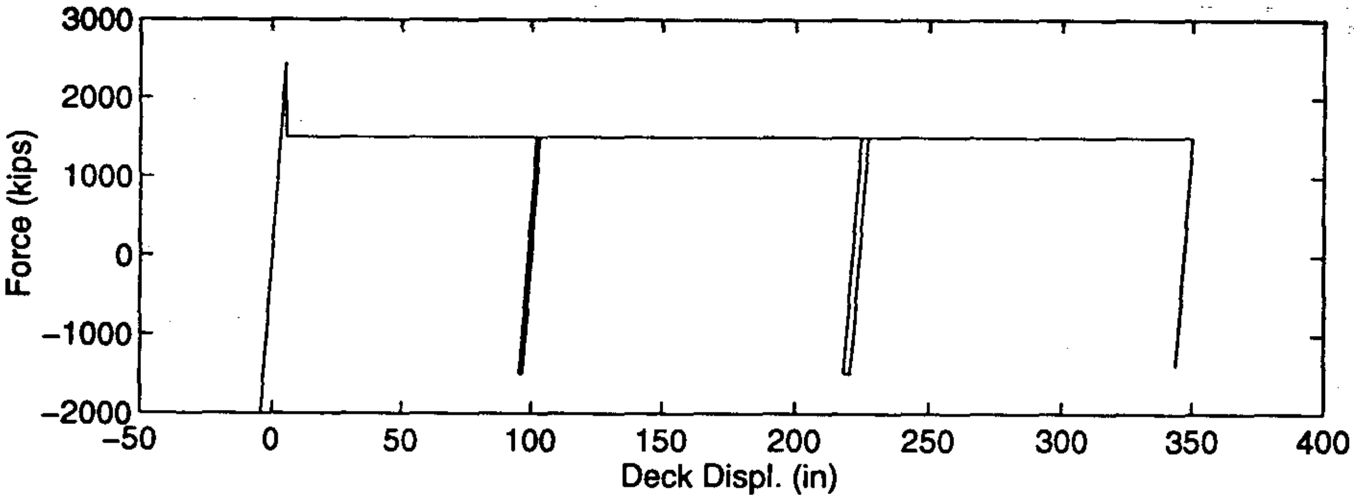

Figure 3.7: B/EPP Resisting Force vs. Deck Displacement, Series 95' Wave Attack

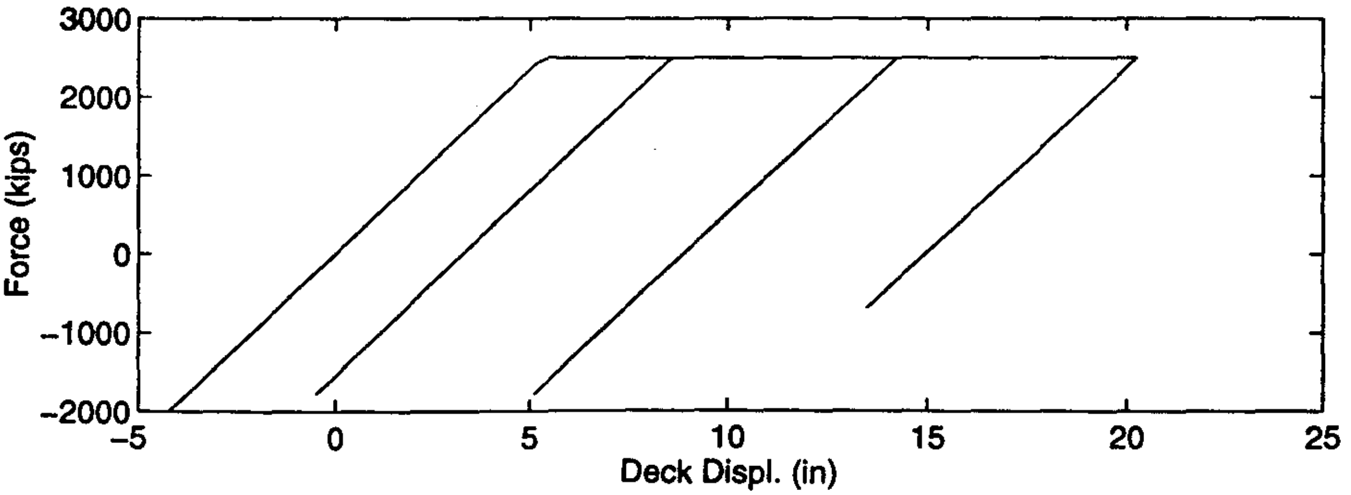

Figure 3.8: EPP Resisting Force vs. Deck Displacement, Series 95' Wave Attack

4.0 CONCLUSIONS

After reviewing the results of the analyses of the two structural behavior models, it should become apparent that the threat from a single wave to a B/EPP structure, or in fact to any structure which undergoes a drop in strength with first member failure, is very serious. The single event can easily take the platform beyond whatever ductile capacity it may have. For the EPP structural system, the platform stands a much better chance of surviving overload from a single wave attack and from some series wave attacks. The improvement in structural performance between the EPP and the B/EPP systems cannot be neglected; the ability of the EPP to absorb some inelastic deformation without losing strength is of great importance when considering time-dependent loads.

From a design standpoint, it would appear that improving the horizontal framing of these jacket structures improves their robustness to a significant degree, even though their effective yield strength has not changed. This improving of ductile capacity may definitely be worth the extra cost and effort of additional members, especially when considering the consequences of failure.

This difference between static and dynamic performance should be recalled when efforts are being taken to requalify structures which may be marginal. Simply because a structure has been subjected to overload does not mean that it has failed completely. It may in fact survive in a condition which may be rehabilitated, or at the very least prevent a very costly and dangerous catastrophic collapse.

5.0 BIBLIOGRAPHY

1. American Petroleum Institute, "API RP 2A-WSD, Section 17, Assessment of Existing Platforms," API, April 1, 1994.
2. Bea, R. G., "Wind and Wave Forces on Marine Structures," Class notes for CE205B, UC Berkeley, Fall 1995.
3. Bea, R. G., Mortazavi, M., and Stear, J. D., "Screening Methodologies for Use in Platform Assessments and Requalifications," UC Berkeley CE MTMG, November 1995.
4. Bea, R. G., and Young, C., "Loading and Capacity Effects on Platform Performance in Extreme Storm Waves and Earthquakes," Offshore Technology Conference, OTC 7140, 1993..
5. Brebbia, C. A., and Walker, S., Dynamic Analysis of Offshore Structures, Newnes-Butterworths, London, 1979.
6. Chopra, A. K., Dynamics of Structures: Theory and Applications to Earthquake Engineering, Prentice Hall, Englewood Cliffs, New Jersey, 1995.
7. MATLAB v.4.2c, Mathworks
8. Rodenbusch, G., "Random Directional Wave Forces on Template Offshore Platforms," Offshore Technology Conference, OTC 5098, 1986.
9. Ruhl, J. A., "Offshore Platforms: Observed Behavior and Comparisons with Theory," Offshore Technology Conference, OTC 2553, 1976.